Boundary-Layer Meteorology (2023) 188:389–418
https://doi.org/10.1007/s10546-023-00818-w

RESEARCH ARTICLE

The Role of Vertical Diffusion Parameterizations in the Dynamics and Accuracy of Simulated Intensifying Hurricanes

Leo Matak[1] · **Mostafa Momen**[1]

Received: 12 February 2023 / Accepted: 6 June 2023 / Published online: 12 July 2023

Abstract
Rotation in hurricane flows can significantly impact the dynamics and structure of the turbulent boundary layer. Despite this unique feature of hurricane boundary layers, the current planetary boundary layer (PBL) schemes in weather models are neither specifically designed nor comprehensively tested for intensifying hurricane flows. The objective of this paper is to bridge this knowledge gap by characterizing the role of vertical diffusion depth and magnitude in simulated hurricane intensity, size, and track. To this end, five major hurricane cases undergoing an intensification period are simulated using two widely used local and non-local PBL schemes in Weather Research and Forecasting (WRF) model. In total, eighty WRF simulations are conducted by varying the grid resolution, PBL scheme, eddy diffusivity depth and magnitude, and PBL height. By decreasing the existing vertical diffusion depth and magnitude, on average, ~ 38 and ~ 24% improvements in hurricane intensity forecasts were obtained compared to the default models. Hence, the results indicate that the current PBL schemes in WRF are overly diffusive for simulating major hurricanes since they do not account for turbulence suppression effects in rotating hurricane flows. The paper yields new insights into the role of vertical diffusion in simulated hurricane dynamics and provides some guidance to enhance the PBL schemes of NWPs for improved hurricane forecasts.

Keywords Eddy diffusivity · Hurricane simulations · Numerical weather prediction · Planetary boundary layer · Vertical diffusion

1 Introduction

Hurricanes have been the costliest weather disaster in US history by causing billions of dollars in damage and thousands of human lives (Cheikh and Momen 2020; NOAA-NCEI 2021; Romdhani et al. 2022). Hurricanes are projected to become stronger and more destructive in the future (Emanuel 2005; U.S. Global Change Research Program 2017). Only five

✉ Mostafa Momen
mmomen@uh.edu

[1] Department of Civil and Environmental Engineering, University of Houston, Room N134, 4726 Calhoun Road, Houston, TX, USA

Hurricanes since 2005 (Katrina, Harvey, Maria, Sandy, and Ida) caused more than $600 billion inflation-adjusted estimated costs (NOAA-NCEI 2021). For instance, Hurricane Maria (2017) resulted in more than $90 billion in unadjusted costs and left thousands of homes in Puerto Rico uninhabitable, damaged, or destroyed (Pasch et al. 2019). It is thus crucial to improve our understanding and modeling of hurricane flows to be able to accurately forecast them and reduce their associated costs.

Numerical weather prediction (NWP) models provide a strong tool for forecasting hurricanes' intensity, size, and track. Despite the recent advances in the current NWP models for hurricane simulations (Gopalakrishnan et al. 2012; Gall et al. 2013; Elsberry 2014; Cangialosi et al. 2020), they still face difficulties in predicting the rapid intensification (RI) of major hurricanes (Krishnamurti et al. 2005; Ku et al. 2020; DeMaria et al. 2021), which occurs in a growing number of storms (Bhatia et al. 2019). For example, over a 24 h period, Hurricane Patricia intensified by over 90 kt, going from a category 1 hurricane to category 5 (Landsea and Franklin 2013). During that 24 h of the RI period, the National Hurricane Center (NHC) predicted only 30 kt of its intensification. Some possible reasons for this poor performance of NWPs include their coarse grid resolutions (1–30 km) that do not resolve turbulence, particularly in their boundary layer, and their inaccurate physical parameterizations (Bhaskar Rao et al. 2009; Fierro et al. 2009; Jin et al. 2014; Shin and Dudhia 2016; Alimohammadi and Malakooti 2018; Romdhani et al. 2022).

The planetary boundary layer (PBL) plays a central role in hurricane dynamics and simulations. Many factors impact PBL dynamics such as stratification (van de Wiel et al. 2010, 2012; Holtslag et al. 2013; Momen and Bou-Zeid 2017a, b), baroclinicity (Momen et al. 2018; Momen 2022), and unsteadiness (Momen and Bou-Zeid 2016, 2017b). These factors can alter the conventional view of PBLs as an Ekman boundary layer (Stull 1988), e.g., by varying the eddy viscosity profiles due to stratification and baroclinicity, or by unsteady effects caused by the changes in pressure gradient or buoyancy fluxes. Despite many considerable studies of different PBLs (Beare et al. 2006; Ramamurthy et al. 2007; Li et al. 2012; Pan et al. 2014; Momen and Bou-Zeid 2017a, b; Salesky et al. 2017; Salesky and Anderson 2018; Stoll et al. 2020), our understanding of the role of strong rotation in hurricanes in the mean and turbulence dynamics of PBLs is still limited. PBL turbulence plays a vital role in predicting wind shear, which is a major contributor to the overall intensification of hurricanes (Kossin 2017; Zhang et al. 2017; Rios-Berrios and Torn 2017; Zhang and Rogers 2019).

The flow regimes in hurricanes can be characterized by defining the Rossby number (Ro), which is a dimensionless number that describes the ratio of the centrifugal to the Coriolis acceleration. Due to strong rotational effects in hurricanes, the Ro number in hurricane boundary layers (HBLs) is high ($Ro \gtrsim 1$) which makes them significantly different from regular PBLs (Smith and Montgomery 2010; Zhang et al. 2011a; Momen et al. 2021) that have a small Ro number ($Ro \approx 0$). The rotation has been shown to suppress or enhance turbulence production in rotating shear flows similar to stabilization or destabilization in stratified flows (Tritton 1992; Cazalbou et al. 2005; Durbin 2011; Arolla and Durbin 2013). Several previous large-eddy simulations (Worsnop et al. 2017; Momen et al. 2021; Sabet et al. 2022) and observational (Zhang 2010) studies have shown the shift of the energy-containing eddies toward higher wave numbers in HBLs compared to regular PBLs. Despite this evidence that rotation in HBLs can remarkably influence PBLs, the default versions of the current NWP models do not account for the role of rotation in PBL turbulence parameterizations that can significantly impact their hurricane forecasts.

Hurricane simulations are sensitive to the choice of the PBL scheme and its parameters (Kanada et al. 2012; Gopalakrishnan et al. 2013; Zhang et al. 2015, 2020; Li et al. 2023). The storm structure and intensity (Kepert 2012) and hurricane RI (Zhang et al. 2017) are highly

modulated by the selected PBL scheme. For instance, up to 15 m s^{-1} differences in hurricane winds were found among four PBL closures in Pennsylvania State University–National Center for Atmospheric Research Mesoscale Model [MM5; (Braun and Tao 2000)].

Two approaches are often used in NWPs to parameterize vertical turbulent fluxes, known as local and non-local PBL schemes (Stull 1988). In local closures, turbulent fluxes depend only on conditions at that level. In non-local closures, such fluxes depend on known quantities elsewhere in the vertical direction. The Mellor–Yamada–Janjic (MYJ) is a common local PBL scheme used in Weather Research and Forecasting (WRF) model (Janjić 1994). The Yonsei University (YSU) and Medium-Range Forecast Model (MRF) are two common non-local schemes (Hong et al. 2006; Hong 2010). This approach uses a prescribed eddy diffusivity profile and is also known as the K-profile parameterization (KPP).

Several studies showed that the current PBL schemes in WRF overestimate the actual eddy diffusivity in hurricane simulations (Zhang et al. 2011a, 2017; Kepert 2012; Gopalakrishnan et al. 2013; Bu et al. 2017; Zhang and Rogers 2019). For instance, previous hurricane simulations indicated that the Global Forecasting System (GFS) PBL scheme, which is a KPP non-local parameterization, produced eddy diffusivity which was four times greater than the observed values (Gopalakrishnan et al. 2013). After introducing a tuning parameter for the GFS PBL scheme, which reduced the estimated eddy diffusivity, the simulation results improved and the forecasting error was notably reduced (Zhang et al. 2015, 2020). The MYJ scheme was also shown to increase surface friction compared to the YSU in Hurricane Isabel simulations (Nolan et al. 2009b). Observational evidence demonstrates that some of the current conventional vertical diffusion schemes in NWPs overestimate the measured vertical eddy diffusivity in hurricanes (Zhang et al. 2015).

Other than the eddy diffusivity profile, the PBL height in hurricanes can also significantly impact their simulations. For instance, Ma et al. (2018) showed nonlinear effects of the PBL height on the intensification of tropical cyclones (TCs). Furthermore, evidence from observations (Zhang et al. 2011b) and numerical studies (Momen et al. 2021) indicate that in hurricanes the kinematic BL height determined by Reynolds stress flux thresholds is significantly higher than the mixed-layer depth determined by the critical Richardson number (referred to as the thermodynamic PBL height used in the YSU scheme). These studies suggest that the existing NWP models have not properly parameterized PBLs for simulating TCs.

Despite the significant impacts of the PBL schemes on hurricane simulations, the evaluation and adjustment of these parameterizations have not been comprehensively performed for multiple real hurricane forecasts. In particular, our understanding of the impacts of the vertical eddy diffusivity and turbulent PBL height on the evolution and dynamics of real major hurricane simulations is limited. Our objective in this study is to address these knowledge gaps by conducting five different real hurricane simulations using two different types of PBL schemes (one local and one non-local) in the Advanced Research WRF (ARW) model. This goal will be achieved by characterizing the default WRF-ARW model's performance as well as new adjustments applied to its eddy diffusivity and PBL height estimations. Hence, our main research questions are:

- How do the height and magnitude of the vertical diffusion influence the dynamics and structure of real hurricane simulations?
- How can we improve the accuracy of major hurricane forecasts during their intensification period by adjusting the existing PBL parameterizations in WRF-ARW?

The paper is organized as follows. Section 2 provides an overview of the study cases, numerical model description, core formulations, and evaluation metrics. Section 3 answers the aforementioned research questions by extensively discussing and characterizing the impacts

of the PBL scheme adjustments on hurricane intensity, size, inflow layer, wind profiles, and forecasting accuracies of real hurricane simulations. Finally, Sect. 4 provides a summary of the key findings of this study.

2 Methods

2.1 Hurricane Case Selection

In view of the objective of this study, we focused on categories 4–5 hurricanes according to the Saffir–Simpson scale (Simpson and Saffir 1974). Our subject group consists of five major hurricanes. The selected hurricanes are Igor, Maria, Dorian, Lorenzo, and Iota. Table 1 provides a summary of the chosen hurricanes along with their formation/dissipation date, our simulation period, and maximum observed intensity during the simulation period.

The selected TCs formed in the Atlantic Ocean. The track of the considered hurricanes is shown in Fig. 1. In this figure, the dotted lines represent the observed best track, and bolded parts of the lines display our simulation periods. Note that the simulation periods are chosen based on the intensification of the hurricanes such that the wind intensities increase over

Table 1 Summary of the selected hurricanes in this study. The intensity data are extracted from the best-observed values of the National Hurricane Center (NOAA-NHC 2021)

Hurricane [category]	Formation–dissipation	Simulation period	Max intensity (ms^{-1})
Igor [4]	Sep. 8–23, 2010	Sep. 11–14	67 m s^{-1}
Maria [5]	Sep. 16- Oct. 2, 2017	Sep. 17–19	72 m s^{-1}
Dorian [5]	Aug. 24- Sep. 10, 2019	Aug. 30- Sep. 2	82 m s^{-1}
Lorenzo [5]	Sep. 23- Oct. 7, 2019	Sep. 25–27	64 m s^{-1}
Iota [4]	Nov. 13–18, 2020	Nov. 15–16	69 m s^{-1}

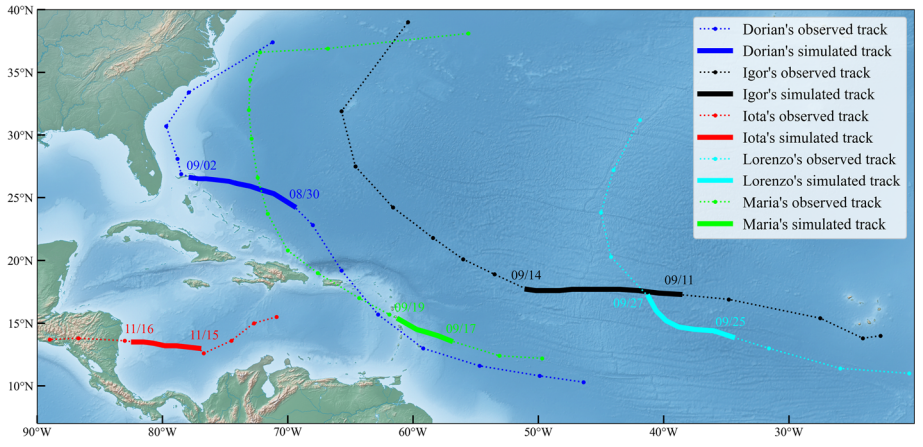

Fig. 1 The best-observed track of the five considered hurricanes in this study. Bolded portions of the track represent the periods of conducted simulations

17 m s^{-1} in 36 h. Furthermore, the starting date has been chosen such that the hurricanes are at least category 1 and at the end of the simulation period, they become category 4 or 5.

2.2 Modeling Framework and Formulations

In this study, hurricane simulations were conducted using the WRF-ARW mesoscale model, version 4.2.2, which is developed and maintained by the National Center for Atmospheric Research (NCAR). The code solves fully compressible, non-hydrostatic Euler equations. It is a finite difference model based on terrain-following hydrostatic vertical coordinates, where the top of the model is defined by a constant pressure surface. In the horizontal directions, the code uses the Arakawa-C type staggering method (Skamarock, et al. 2008). The time integration is done using the time-split 3rd-order Runge–Kutta scheme, which includes different time steps for acoustic and gravity waves. The WRF-ARW model includes multiple options for the physics suite. In our simulations, we used the WRF Single-Moment 6-class scheme for microphysics (Hong and Lim 2006), the Noah land Surface Model for surface physics (Ek et al. 2003), and the Kain-Fritsch scheme for cumulus parameterization (Kain 2004).

The vertical diffusion in mesoscale WRF-ARW simulations is handled by the PBL schemes. When a PBL scheme is employed, all other vertical mixing is disabled. The PBL is responsible for parameterizing the sub-grid scale unresolved vertical turbulent fluxes of momentum, heat, and other scalars throughout the whole 1D vertical column, including both the boundary layer as well as the free atmosphere.

We used a local and a non-local PBL scheme to conduct the simulations in WRF-ARW. For the non-local PBL parameterization, the YSU scheme is used in this study, which is the recommended model for TC simulations by the WRF-ARW guideline (Wei et al. 2019). For the local PBL parameterization, we employed the MYJ scheme, which is a widely used method for simulating hurricanes (Nolan et al. 2009b; Li et al. 2020; Rajeswari et al. 2020). Note that we expect that any other PBL scheme that does not account for turbulence suppression/enhancement effects due to strong rotation should have a similar performance in predicting the major hurricane's intensity as the selected schemes. In fact, we tested this by comparing the results of the default MYJ scheme with another more sophisticated version, i.e., Mellor–Yamada–Nakanishi–Niino (MYNN 3.0) PBL scheme (Chen 2022), and noticed a small difference in intensity predictions of three simulated hurricanes (not shown).

To examine the performance of the default PBL schemes in WRF-ARW for simulating real major hurricanes, we will alter both the magnitude and depth of the vertical eddy diffusion. YSU is known as a non-local PBL scheme because not only it considers contributions from neighboring or adjacent grid cells, but also it has additional terms which represent deeper vertical fluxes stretching from surface layers up to the top of the PBL. In the non-local YSU scheme, the eddy diffusivity is prescribed as a polynomial function as:

$$K_m(z) = C_k \kappa w_s z \left(1 - \frac{z}{h}\right)^p, \tag{1}$$

where K_m is the momentum eddy diffusivity, κ is the von Kármán constant ($\kappa = 0.4$), w_s is the mixed-layer velocity scale, p is an exponent for the profile shape (in YSU, $p = 2$), h is the height of the PBL which in YSU is determined based on the critical Richardson number, and z is the height above the ground. In this formula, C_k is our newly defined parameter that we will use to control the vertical diffusion magnitude in the PBL.

On the other hand, MYJ is a 1.5-order local turbulence closure scheme that only considers the contributions from adjacent cells, their mean values, and their gradients (Mellor and

Yamada 1982; Janjić 1994; Janjic 2002). It belongs to the turbulent kinetic energy (TKE) family of PBL schemes because it solves the prognostic TKE equations. In the local MYJ PBL scheme, the eddy diffusivity is determined as:

$$K_m = C_k q l S_M, \tag{2}$$

where q denotes the TKE, l represents a master turbulent mixing length scale, and S_M represents a function of the dimensionless shear. In our simulations, the vertical eddy diffusivity for heat (K_h) is not assumed to be equal to K_m. The PBL schemes handle K_h separately either based on the Prandtl number (for YSU) or the TKE prognostic equations (for MYJ). Some of our hurricane simulation results show a similar trend to observational estimates (Zhang and Drennan 2012) in which both K_m and K_h are comparable, but K_h is smaller than K_m for the considered hurricanes.

For modulating the vertical diffusion height in these schemes, we eliminate the vertical diffusion at higher elevations by setting it to zero above specific levels as $K_m\left(z \geq z_{lvl_x}\right) = 0$, where z_{lvl_x} denotes the elevation of level x above the surface. Based on the defined vertical levels in this study, we cut off K_m at and above two different heights $z_{lvl4} \sim 261$ m and $z_{lvl_6} \sim 536$ m, which hereafter are referred to as $K_{m\_}lvl_4$ and $K_{m\_}lvl_6$, respectively. This has a similar impact on the results as changing the PBL height which will be shown in the next section. We also present another set of simulations where we directly alter the PBL height, h in Eq. (1), in the YSU scheme.

These new adjustments will only be applied to strong wind regions where the *Ro* is high, and we will not modify the environmental low-wind field regimes where the effects of rotation are small. To this end, we confine the full application of the changes of the control parameter C_k as well as the vertical diffusion depth to only regions where the surface wind speed is larger than 10 m s^{-1}. This will cover modifying the TC vortex region of the simulation domain. As an example, our approach is formulated in Eq. (3), where we alter the height of the PBL (h) using the following piece-wise linear function:

$$h(wspd_{10}) = \begin{cases} h, & wspd_{10} \leq 5\,\text{m s}^{-1} \\ \left\{h + \left[\frac{wspd_{10}-5}{5}\right] * (PBLH - h)\right\}, & 5\,\text{m s}^{-1} < wspd_{10} < 10\,\text{m s}^{-1} \\ PBLH, & wspd_{10} \geq 10\,\text{m s}^{-1} \end{cases} \tag{3}$$

where *PBLH* denotes the modified PBL height (= 250 or 1000 m). Satellite and Stepped Frequency Microwave Radiometer (SFMR) observed values of surface wind speeds of major hurricanes (not shown) indicate that hurricane vortex (where the Rossby number is considerable) extends ~ 500 km from the center where the winds become ~ 10 m s^{-1}. In order to avoid sudden jumps in the vertical diffusion depth or magnitude, we defined a buffer transition zone from 5 to 10 m s^{-1} in Eq. (3) where the changes are applied linearly. In this formula, the PBL heights remain unchanged for low wind speeds smaller than 5 m s^{-1}, and they linearly increase or decrease to the specified *PBLH* such that the PBL height is entirely changed to the *PBLH* for surface winds greater than 10 m s^{-1}. The resulting changes to a PBL height based on the magnitude of the surface wind speed for *PBLH* = 250 m are shown in Fig. 2. As the figure indicates, the default PBL height (Fig. 2a) for hurricane vortex region (green and red colors in Fig. 2b,d) is changed to 250 m height (see blue colors near the hurricane vortex in Fig. 2c and compare with Fig. 2a) while the PBL height in low-wind environmental wind field regimes remains unchanged. We employ a similar approach for applying the vertical diffusion magnitude changes via the C_k parameter based on a piece-wise surface wind speed function akin to Eq. (3). Note that the choices of the PBL height of 250 and 1000 m, and the vertical diffusion limiter elevations of 263 and 536 m are consistent with the previous

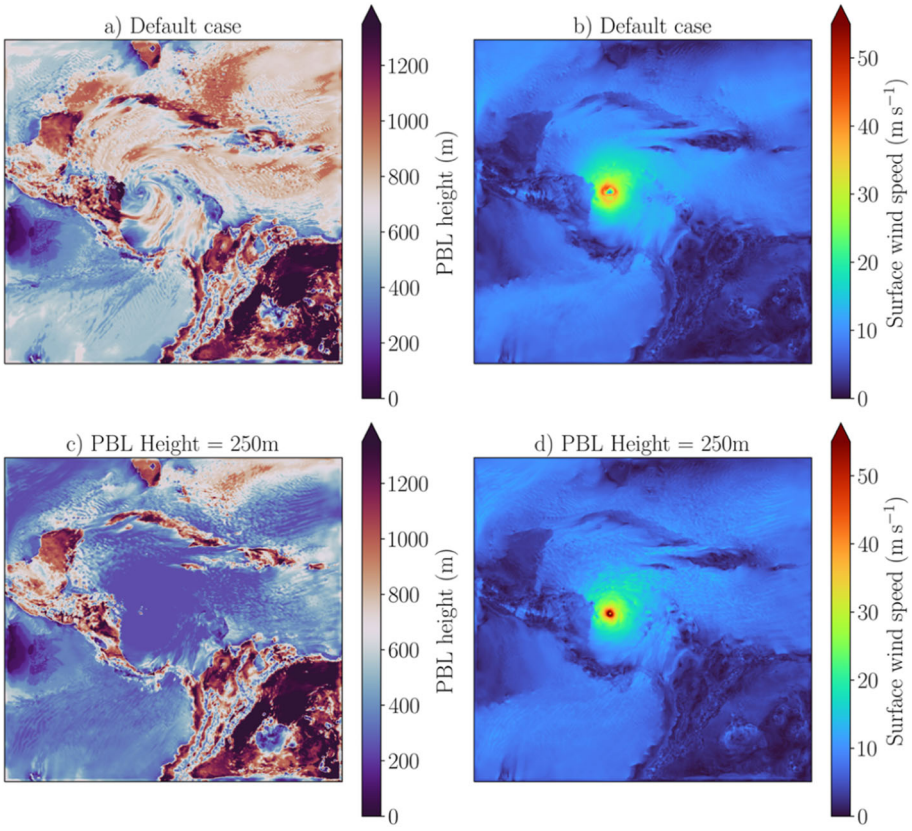

Fig. 2 The implementation of changing the PBL height of (top) the default YSU scheme case to (bottom) PBLH = 250 m following Eq. (3), for Hurricane Iota, at a later stage of the simulation (~ 30 h)

observational and numerical estimations of the mixed layer depth in different hurricanes that resulted in values between 250 and 1000 m (Nolan et al. 2009a; Zhang et al. 2009).

2.3 Suite of Simulations

First, we conducted a suite of simulations to examine the grid resolution sensitivity of the default PBL schemes in WRF-ARW. Three different grid size simulations were carried out for each of the hurricanes, and each of the PBL schemes. For this purpose, we ran [3 grid sizes] × [5 hurricanes] × [2 PBLs] = 30 simulations. Table 2 provides detailed information about our entire suite of simulations. We define a naming convention (last column in Table 2) for the conducted cases that will be used hereafter. For example, Iota_YSU_8km represents Hurricane Iota simulation conducted with the YSU scheme and 8 km horizontal grid resolution.

The second suite of simulations characterizes the impacts of changing the height of the vertical turbulent diffusion on hurricane dynamics. To this end, we constrained the eddy diffusivity depth by varying the level at which the momentum exchange coefficient is set to be zero ($K_m = 0$) in the model. This time we ran [2 K_m height modifications] × [5 hurricanes]

Table 2 The list of conducted suites of WRF-ARW simulations

Hurricanes	Type of analysis	Case Variations			Naming Convention and PBLs Used
Igor Maria Lorenzo Dorian Iota	1) Grid sensitivity test	**2 km**	**8 km**	**32 km**	**HN**_YSU_**X**km
					HN_MYJ_**X**km
	2) Vertical diffusion depth variations (Turbulent BL height)	$K_m\_lvl_4$	$K_m\_lvl_6$		**HN**_$K_m_lvl_X$_YSU
					HN_$K_m_lvl_X$_MYJ
	3) PBL Height	*PBLH*_250	*PBLH*_1000		**HN**_*PBLH*_***X***YSU
	4) Vertical diffusion magnitude variations	C_k = 0.2	C_k = 5.0		**HN**_C_k_***X***_YSU
					HN_C_k_***X***_MYJ

HN is a placeholder for the hurricane name which can be either Igor, Maria, Dorian, Lorenzo, or Iota. The total number of runs is [5 hurricanes] × { [2 PBLs] × [3 grid sensitivity] + [2 PBLs] × [2 K_m height modifications] + [1 PBL] × [2 PBL heights] + [2 PBLs] × [2 momentum exchange variations]} which tallies to 80 runs

× [2 PBLs] = 20 simulations. In this set of simulations, the precise value of the height of the HBL was not directly changed; nevertheless, by limiting the depth of the mixing processes, we effectively controlled the height of the turbulent boundary layer. This will be shown by the third suite of simulations in which we explicitly modify the PBL height defined in Eq. 1 of the YSU scheme. To this end, we altered the default PBL height to 250 and 1000 m which led to 10 new simulations. For the naming convention, e.g., Iota_$K_m_lvl_6$_YSU represents the Iota simulation with the YSU scheme in which K_m is set to zero at vertical level 6 and above.

The fourth suite of simulations determines the role of the magnitude of the eddy diffusivity in hurricane simulations. To this end, we varied the values of the newly added control parameter C_k in Eqs. (1–2) by a factor of 5. Thus, we compare the default unmodified WRF-ARW simulations with runs that had their momentum exchange coefficients increased or decreased by a factor of 5. The number of simulations we ran was [2 momentum exchange variations] × [5 hurricanes] × [2 PBLs] = 20. In total, we conducted 30 + 20 + 10 + 20 = 80 WRF-ARW hurricane simulations in this study.

2.4 Evaluation Metrics

For calculating the accuracy of our simulations, we employed three metrics. For computing the hurricane wind intensity, the mean absolute percentage error (MAPE) is used. This metric normalizes the wind speed and, thus, we can compare different hurricane categories and intensities with a unified dimensionless criterion (Romdhani et al. 2022). Hence, the wind intensity error is calculated as follows:

$$MAPE_{\text{intensity}} = \frac{100\%}{n} \sum_{i=1}^{n} \left| \frac{V_{For}^{i} - V_{Obs}^{i}}{V_{Obs}^{i}} \right|, \tag{4}$$

where V_{Obs}^{i} denotes the best observed wind intensity at timestep t_i, V_{For}^{i} represents the forecasted wind intensity (i.e., the maximum wind speed at 10 m height) at timestep i, and n shows the number of available observation samples during the simulation period. For observations, the U.S. NHC best track and intensities reported data are used, which have been evaluated against a combination of aircraft, dropwindsonde, and satellite observations (Kidder et al. 2000; Klotz and Uhlhorn 2014; Huffman et al. 2015). Hence, the values of

V^i_{Obs} are obtained from the NHC best track reports, which have a temporal resolution of 6 h (i.e., t_{i+1}-$t_i = 6$ h). The intensities data of NHC are best maximum 1-min sustained 10 m wind speed. The value of V^i_{For} from the WRF model is a maximum instantaneous wind speed at 10 m elevation outputted at the same time step of the NHC data. This comparison is a common practice in hurricane forecasting studies (Nolan et al. 2009b; Green and Zhang 2015; Shen et al. 2016, 2020; Liu et al. 2017).

For track error, since there is no universal length scale for normalization, we used the mean absolute error (MAE) between the forecasted and observed hurricane positions. When calculating the MAE for track, the difference between the coordinate points was converted into distance in kilometers by using the Haversine formulae (Choudhury and Das 2017). The Haversine formula determines the distance between two points on a sphere in kilometers if a pair of longitude and latitude values are given. Thus, the MAE for track is calculated as follows:

$$MAE_{track} = \frac{1}{n}\sum_{i=1}^{n} \text{Haversine}\left(\Omega^i_{For}, \Omega^i_{Obs}\right), \tag{5}$$

where Ω(lon, lat) represents a function of longitude and latitude of the hurricane eye at a given timestep i. Ω^i_{Obs} in Eq. 5 represents the best observed hurricane position whereas Ω^i_{For} denotes the forecasted hurricane position. Ω^i_{For} is obtained by finding the longitude and latitude of the grid point with the lowest sea-level pressure (SLP) over the simulated domain. The last employed metric is the MAE for minimum SLP, which is calculated as:

$$MAE_{SLP} = \frac{1}{n}\sum_{i=1}^{n} \left|\min(SLP^i_{For}) - \min(SLP^i_{Obs})\right|, \tag{6}$$

where $\min(SLP^i_{Obs})$ is provided by the reported data from NHC. Note that using only these three metrics may not reveal a thorough sensitivity of the simulation results to other parameters such as turbulence dynamics. However, measuring turbulent quantities in hurricanes is challenging since TCs evolve rapidly over the Ocean where available observations are limited. Hence, similar to other studies (Davis et al. 2010; Zhang et al. 2015) we use the NHC reported data for calculating these error indices to evaluate the performance of WRF in simulating hurricanes.

3 Results

3.1 Grid Sensitivity Test for the Chosen Hurricanes

First, we conducted a grid sensitivity test for both considered PBL schemes in their default settings to determine their grid dependence and to maintain computational efficiency for the next runs. The default model runs were carried out for all five hurricanes using three different grid resolutions. Figure 3 shows the average statistics of the forecasting errors for these five hurricanes compared to the best-observed data. As the figure indicates, an overall improvement in the forecasting skill with increasing horizontal grid resolution can be noticed consistent with previous studies (Hill and Lackmann 2009; Bhaskar Rao et al. 2009; Davis et al. 2010; Alimohammadi and Malakooti 2018). In particular, ~ 34.9% improvement for the intensity [(*MAPE* 32 km–*MAPE*8 km) × 100%/*MAPE* 32 km] and ~ 4.4% improvement

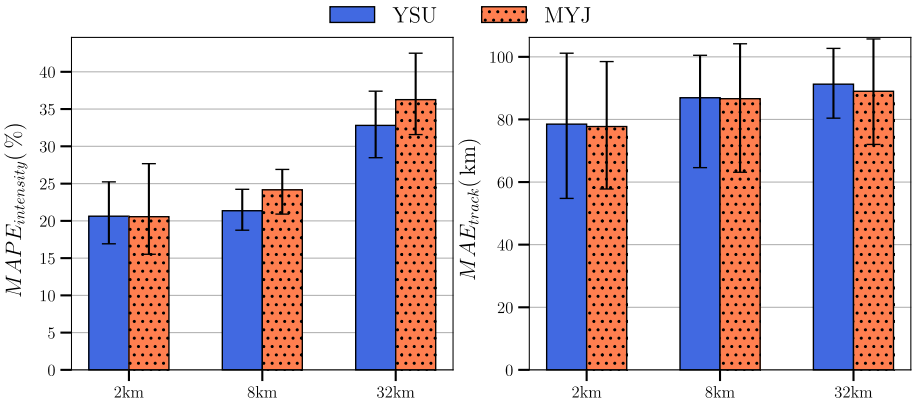

Fig. 3 Grid sensitivity analysis of the default WRF runs for both YSU and MYJ PBL schemes. The left panel shows normalized wind intensity errors along with their 20th and 80th percentile error bars. The right panel shows absolute track errors along with their 20th and 80th percentile error bars. Errors are averaged over all five hurricanes and the entire simulation period

for track [(*MAE* 32 km–*MAE* 8 km) × 100%/*MAE* 32 km] forecast of the YSU scheme is achieved when increasing the grid resolution from 32 to 8 km.

As we further increase the grid resolution from 8 to 2 km, the improvement in intensity forecasts becomes smaller (see Fig. 3). Fierro et al. (2009) showed that there is not a significant change in wind intensities forecasts of TCs when increasing the horizontal grid resolution from 5 to 1 km probably since these NWPs do not resolve turbulence. This is consistent with our finding in Fig. 3 (left) that there is ~ 3.4% improvement in intensity errors of the YSU scheme when going from 8 to 2 km horizontal grid resolution which is less than the achieved improvement from 32 to 8 km. However, we note that the computational cost and required disk storage of 2 km resolution simulations are substantially increased compared to 8 km runs, and exceed our current capacities. Hence, we conducted the new modified simulations with the 8 km grid resolution to save computational and storage resources while providing sufficient accuracy for the main purpose of this study.

It is noteworthy to mention that we also conducted a vertical grid resolution sensitivity by increasing the vertical resolution by ~ 50–80% and changing the distribution of the levels within the PBL for 8 km horizontal grid sizes (not shown). We did not notice any significant differences in the intensity predictions of the considered hurricanes. Hence, the default WRF's vertical levels based on the Hybrid Vertical Coordinate (HVC) system, which covers the atmosphere from 0 to 50 hPa, were used in this paper's runs.

In terms of the comparison between the local and non-local PBL schemes for hurricane wind intensity forecast performance, our analysis indicates that the YSU scheme (recommended by the WRF-ARW guidelines for TC simulations; Skamarock et al. 2021) outperforms the MYJ for both 32 km and 8 km resolutions. This result is consistent with prior studies (Srinivas et al. 2013; Alimohammadi and Malakooti 2018) where they show the YSU scheme forecasts lower intensity errors. At 2 km grid resolution, the difference between the forecasted error for wind intensity of both schemes is small. In terms of the track error, MYJ slightly outperforms the YSU runs (Fig. 3, right panel).

3.2 The Impacts of Changing the Vertical Diffusion Depth on Simulated Hurricane Intensity

To begin with, the effects of changing the K_m depth on hurricane wind intensity will be described. Figure 4 shows the vertical profile snapshots of K_m for all five hurricanes. The snapshots were taken in the middle of the run, and the values of K_m are spatially averaged over grids with high surface wind speeds. Black lines represent the simulation runs without any modifications, and their vertical profiles agree with previous studies (e.g., Kepert 2012; Bu et al. 2017). Blue lines are vertical profiles with the imposed vertical diffusion limiter at height $h \sim 260$m, or in our model configuration at the 4th vertical level ($K_m\_lvl_4$). For the green lines, the vertical diffusion limiter is imposed at level 6, $K_m\_lvl_6$, which corresponds to $h \sim 535$m. By introducing the vertical diffusion limiter, we have effectively reduced the vertical momentum mixing to zero after a certain height. Thus, the turbulent boundary layer height is decreased since vertical mixing becomes zero above these levels. In the next sections, we will show that this approach provides comparable results with another suite of simulations where we directly change the PBL height for the YSU scheme. This approach allows us to employ a similar method for controlling the turbulent PBL height both in local and non-local PBL schemes.

The changes in K_m profiles in the YSU runs show that, below the modulated level, K_m mostly follows the default case while above that it becomes zero as expected (see top panels of Fig. 4). On the other hand, for the MYJ runs while above the modulated level K_m becomes

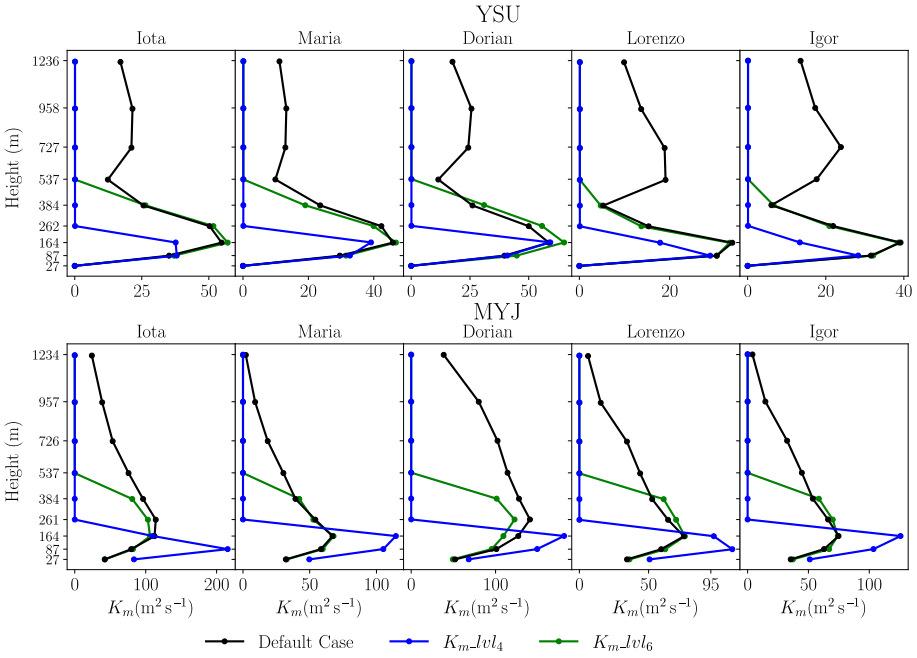

Fig. 4 Vertical profiles of all five simulated hurricane eddy diffusivity for both (top) YSU and (bottom) MYJ schemes. The profiles are extracted from the middle of simulations. The black lines represent the default simulation runs without modifications. Blue and green lines are modified runs with the vertical diffusion limiter set at vertical levels 4 and 6

zero below that some divergence from the default unmodified runs is observed (compare the blue/green lines with the black line in bottom panels of Fig. 4). The reason for this is due to the MYJ scheme being a TKE based method which evolves nonlinearly in time as the simulations progress while in YSU the K_m employs a priori prescribed profile shape (see Eq. 1). In MYJ, the K_m profile is determined from solving the TKE prognostic equations. Hence, while at the beginning of the simulations, the K_m values of MYJ below the modulated level match the default unmodified runs, as time evolves, they start diverging from the default cases (see supplementary Fig. S1). This is because the imposed K_m height limitation modulates the TKE magnitude and its temporal evolution which consequently impacts the turbulent mixing and K_m values in the MYJ scheme.

Altering the vertical diffusion depth can significantly impact the simulated hurricane intensity. Figure 5 shows the horizontal wind speeds at $z \sim 500$ m (corresponding to the pressure of 950hPa). Figure 5 indicates how changing the depth of K_m can remarkably influence the wind speed magnitudes. When we limit the depth of the K_m to ~ 260 m ($K_m\_lvl_4$), the wind intensity significantly increases compared to the default YSU runs (compare darker red colors in the left panels of Fig. 5 to the right panels). For instance, Hurricane Maria simulations indicate $\Delta V_{Max,Maria} = \mathrm{Max}\left(V_{Maria\_Km\_lvl4\_YSU}\right) - \mathrm{Max}\left(V_{Maria\_Default\_YSU}\right) = 27\ \mathrm{m\ s^{-1}}$ maximum wind speed difference between the reduced vertical diffusion depth and default YSU runs, and similarly for Hurricane Igor $\Delta V_{Max,Igor} = 31\ \mathrm{m\ s^{-1}}$. This is because decreasing the vertical diffusion height reduces the overall turbulent friction and turbulent momentum exchange in the HBL and intensifies the hurricanes (Gopalakrishnan et al. 2013).

The alterations in the vertical diffusion depth can also impact the minimum SLP values. Figure 5 depicts the SLP isobars as thick black lines. A notable difference in pressure field can be found in Hurricane Iota runs, where the default case's minimum SLP is $SLP_{Min} = 958$hPa compared to the $K_m\_lvl_4$ run which results in $SLP_{Min} = 918$hPa, leading to a difference of $\Delta SLP_{Min,Iota} = 40$hPa. Having such a large difference in pressure gradients leads to remarkably different wind intensities in hurricanes. This can be seen from the simplified momentum equation $\partial p / \partial r \sim u_\theta^2 / r$ where p denotes the pressure, r represents the distance from the hurricane eye, and u_θ denotes the tangential wind velocity. Similar results for changing the vertical diffusion depth on wind intensity and SLP of simulated hurricanes were found for the MYJ runs. For more details about the MYJ cases, please refer to Fig. S2 in the supplementary material. Furthermore, a similar trend was observed when explicitly changing the PBL height in the YSU scheme. Decreasing the default PBL height to 250 m, intensifies the considered hurricanes akin to $K_m\_lvl_4$ runs, while increasing the PBL height to 1000 m increases turbulent friction and diminishes hurricane intensification (please refer to supplementary Fig. S3 for more details).

3.3 The Impacts of Changing the Vertical Diffusion Magnitude on Simulated Hurricane Intensity

In the last suite of WRF-ARW simulations, we characterize the impacts of changing the vertical diffusion magnitude on the intensity of simulated hurricanes. As previously noted, in Table 1, we introduced a C_k parameter to control the magnitude of the vertical momentum eddy mixing (see Eqs. 1, 2). These new modifications can be seen in Fig. 6, where the black lines are for the default, unmodified runs, and the blue and red lines represent $C_k = 0.2$ and $C_k = 5.0$ runs, respectively.

Modifying the momentum and heat exchange coefficients near the sea surface significantly impacts the formation of TCs due to air-sea interactions. Altering the exchange coefficients

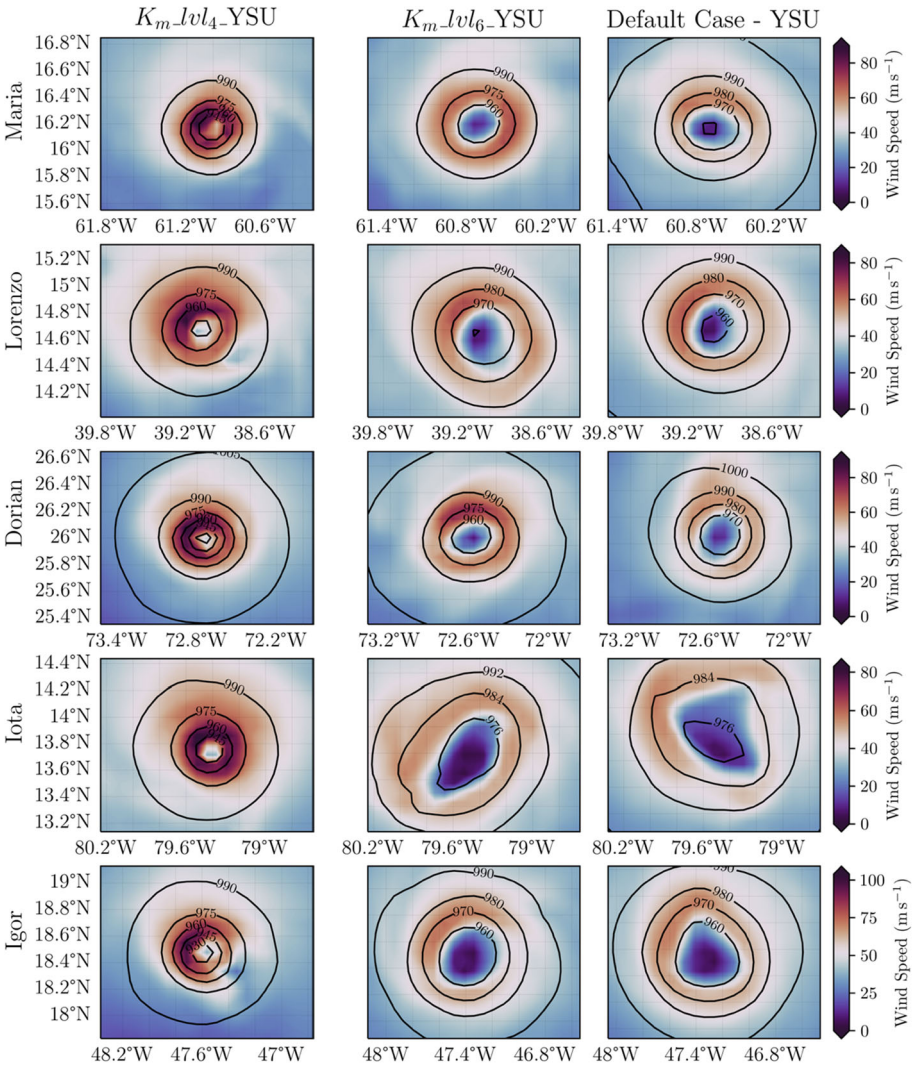

Fig. 5 Wind contours of instantaneous horizontal wind speeds at $z \sim 500$ m for five YSU simulated hurricanes. Columns from left to right: YSU vertical diffusion limiter set at $K_m\_lvl_4$, vertical diffusion limiter set at $K_m\_lvl_6$, and finally the default YSU runs. Black contour lines represent isobars of SLP

of thermal fluxes (e.g., reducing the thermal mixing in the eye region) could lead to a rapid decay of the hurricane vortex. Therefore, to properly maintain the storm development while changing the magnitude of the vertical diffusion, we kept the K_m unchanged at the atmospheric surface layer, which is approximately at $z \lesssim 100$ m (the first two vertical grid points in our configuration), and modified it only above it at heights where $z \gtrsim 100$ m. While modifying the turbulent vertical mixing in the surface layer would not allow the TC to form properly, modifying it above the surface layer allowed for the necessary convection of heat and momentum to occur for TC's inner structure to form.

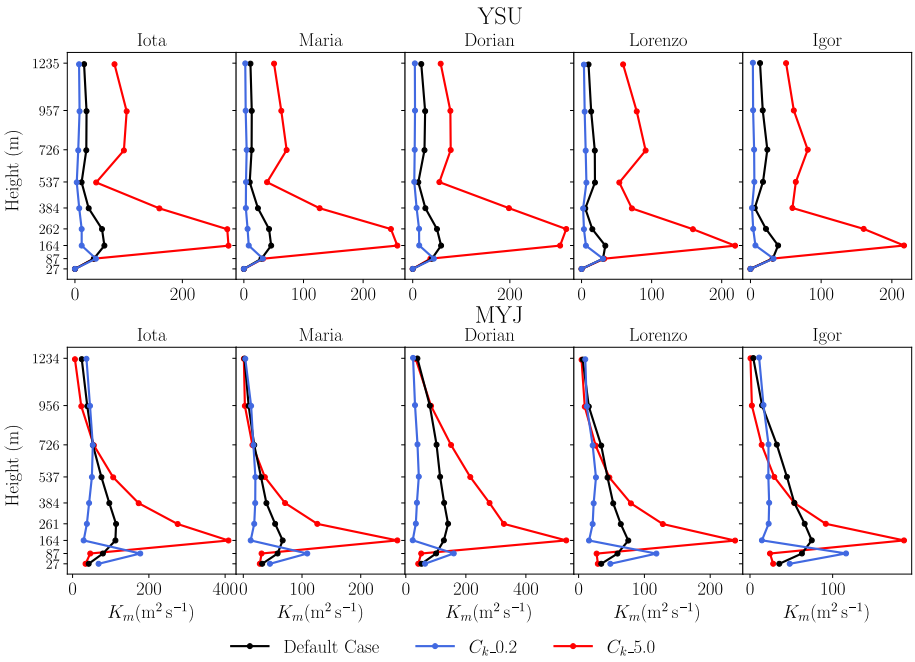

Fig. 6 The vertical profiles of all five simulated hurricane momentum exchange coefficients for (top) YSU and (bottom) MYJ runs. The profiles are extracted from the middle of simulations. The black lines represent the default simulations without modifications. The blue and red lines represent the simulation runs with modified momentum exchange coefficient magnitude $C_k = 0.2$ and $C_k = 5.0$, respectively

The C_k parameter is thus adjusted to control the mixing inside the HBL using this approach as shown in Fig. 6. Adding the C_k control parameter with this approach (Fig. 6) remarkably influences TC's intensity and structure, which will be shown later. Similarly, as in Fig. 4, the MYJ runs slightly diverge from the unmodified runs at the surface layer (the first two vertical nodes) for the same reason as explained earlier (i.e., the nonlinear evolution of the TKE equation), while the YSU modified runs match the default runs at the first two vertical nodes since a priori prescribed K_m profile (Eq. 1) is used for these cases.

Altering the magnitude of the vertical diffusion can significantly impact hurricane vortex intensity. Figure 7 shows the contours of radius-height cross sections of the tangential and radial wind velocities for Hurricanes Lorenzo and Igor. The left columns are wind velocities from reduced eddy diffusivity simulations ($C_k = 0.2$ in Eq. 1), the middle columns depict the default simulation runs, and the right columns display the results obtained with increased vertical diffusion (C_k_5.0 runs). Figure 7 indicates that as the magnitude of the imposed eddy diffusivity is decreased, the tangential wind velocity (u_θ) contours intensify for both YSU and MYJ runs (compare darker red colors of left columns with the lighter red colors in the right columns). As such, Hurricane Lorenzo reaches a maximum tangential wind velocity of $\max\left(u_{\theta,Lorenzo\_Ck\_0.2}\right) = 77.3\,\mathrm{m\,s^{-1}}$ which is higher than the maximum u_θ of the default run about $\Delta\max(u_{\theta,Lorenzo}) = 19.6\,\mathrm{m\,s^{-1}}$. Similarly in Hurricane Igor runs, the maximum tangential wind velocity for C_k_0.2 modification is $\max\left(u_{\theta,Igor\_Ck\_0.2}\right) = 81.3\,\mathrm{m\,s^{-1}}$, resulting in a difference of $\approx 9.9\ \mathrm{m\,s^{-1}}$ when compared to the default run. On

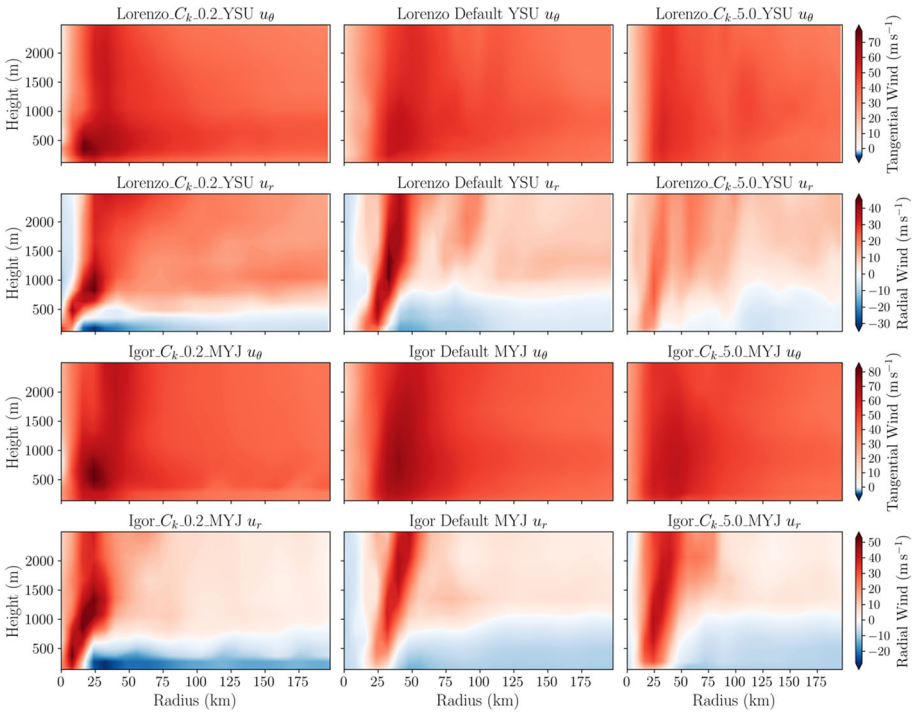

Fig. 7 Radius–height cross sections of the tangential and radial wind velocity contours for Hurricanes Lorenzo (YSU PBL) and Igor (MYJ PBL) runs after 25 h of simulation. Columns from left to right depict decreased eddy diffusivity C_k_0.2, default run, and increased eddy diffusivity C_k_5 simulations, respectively

the other hand, increasing the vertical momentum exchange magnitude (C_k_5.0) results in lower maximum tangential wind intensities in both cases.

The radial wind velocity profiles, which represent the hurricane inflow near the surface, yield a similar trend. As the vertical diffusion magnitude is decreased, the depth of the inflow layer, which is caused by the surface friction, reduces while the magnitude of the inflow increases (compare the darker blue contours of the left columns with lighter blue contours of the middle and right columns in Fig. 7). In particular, the difference between the radial velocity (u_r) of the reduced eddy diffusivity and default runs for Hurricanes Lorenzo and Igor simulations is $\approx 17\,\mathrm{m\,s^{-1}}$ and $20\,\mathrm{m\,s^{-1}}$, respectively. This shallower but stronger inflow layer intensifies the hurricane vortex for reduced vertical eddy diffusivity cases (Gopalakrishnan et al. 2013, 2021). Similar results were found for other hurricane cases as well as with changing the PBL height (see, e.g., supplementary material Figs. S4 and S5).

Decreasing the eddy diffusivity and mixing enhances spinup in the HBL and intensifies the winds in a hurricane. This is analogous to stable stratification in the PBL where the reduced viscosity can lead to low-level jets. This mechanism can be physically explained via a simple single-column model as shown in supplementary Fig. S6. Moreover, previous studies have shown that the maximum potential intensity (MPI) of a storm (Emanuel 1988) is related to the ratio of the enthalpy and surface momentum exchange coefficients. Reducing the eddy diffusivity, effectively decreases the momentum exchange coefficient, increases this ratio, and intensifies hurricanes.

3.4 The Impacts of Modifying the Vertical Diffusion Depth and Magnitude on Simulated Hurricane Size

In addition to TC intensity, vertical diffusion can remarkably modulate the size of hurricanes. Reducing the vertical diffusion depth affects the TC size, as can be seen in the radial profiles of the averaged wind speed in Fig. 8. As the figure indicates, by reducing the eddy diffusivity's effective depth, the radius of the maximum wind (RMW), which represents the eyewall region in a TC, decreases compared to the default runs (compare blue and black lines in Fig. 8). Hence, in addition to a higher maximum wind in reduced vertical diffusion height cases (compare the wind speed peaks in Fig. 8), the size of the TC vortex seems to decrease in such cases compared to the default simulations. This leads to TCs with overall smaller sizes and stronger intensities in decreased eddy diffusivity depths for both considered local and non-local PBL schemes. A similar trend is also observed when explicitly modulating the PBL height of hurricanes in the YSU scheme (see supplementary Fig. S7 for further details).

Similar effects on TC sizes can be deduced from altering the magnitude of the eddy diffusivity. Comparable results to Fig. 8 were found for changing the eddy diffusivity magnitude that can be seen in supplementary Fig. S8. Furthermore, supplementary Fig. S10 depicts the averaged wind profiles as a function of SLP for changing the magnitude of the vertical diffusion by the introduced control parameter, C_k. Supplementary Fig. S10 (S11) indicates that reducing the vertical diffusion magnitude (depth) decreases the minimum SLP and increases the maximum wind intensity compared to the default runs. Thus, decreasing both the vertical

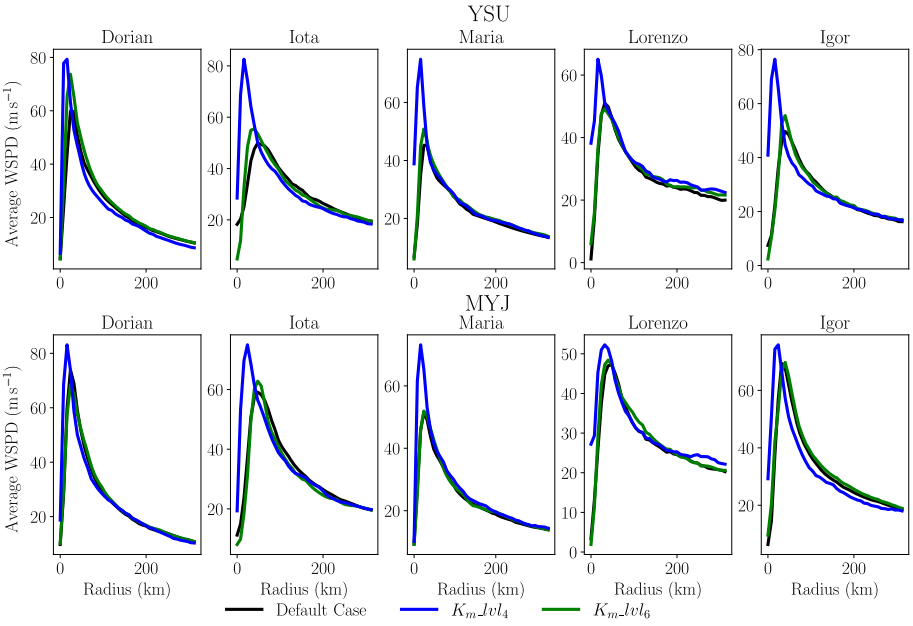

Fig. 8 Averaged wind speed (WSPD) over radius for five simulated hurricanes for (top) YSU, and (bottom) MYJ runs at 500 m height around the middle of the simulations. Black lines represent the default simulation runs without modifications. Blue and green lines are simulation runs with imposed eddy diffusivity depth limiters set at 4th and 6th vertical levels, respectively

diffusion magnitude and depth leads to a stronger and smaller TC vortex for the YSU and MYJ PBL schemes.

To quantify the impacts of the vertical diffusion depth and magnitude on hurricane intensity and size, we calculated the average statistics for the five considered hurricanes from Figs. 8 and S8. These averages are shown as bar plots in Fig. 9 for the YSU (blue bars) and the MYJ (coral bars) PBL schemes. This figure indicates a consistent trend for modulating both the magnitude and depth of the vertical diffusion on TC intensity and size. Both PBL schemes produce higher average maximum wind speeds when their vertical momentum exchange depth (top left panel of Fig. 9) or magnitude (bottom left panel of Fig. 9) is reduced. As such, the YSU runs with $K_m\_lvl_4$ result in an average maximum wind intensity of $\overline{V}_{K_m\_lvl_4\_YSU} = 75.7\,\mathrm{m\,s^{-1}}$, whereas the default runs, on average, generate maximum wind intensity of $\overline{V}_{Default\_YSU} = 57.8\,\mathrm{m\,s^{-1}}$ which leads to a total of $\Delta\overline{V}_{K_m\_lvl_4\_YSU} \approx 17.9\,\mathrm{m\,s^{-1}}$ difference. For the MYJ runs, a notable difference of $\Delta\overline{V}_{K_m\_lvl_4\_MYJ} = 11.5\,\mathrm{m\,s^{-1}}$ is observed. By reducing the magnitude of the eddy diffusivity, the YSU runs produce an increased $\Delta\overline{V}_{C_k\_0.2\_YSU} = 11\,\mathrm{m\,s^{-1}}$ compared to the default runs, whereas the MYJ runs on average generate $\Delta\overline{V}_{C_k\_0.2\_MYJ} = 6.3\,\mathrm{m\,s^{-1}}$ higher wind intensities compared to the default runs. These results indicate that modulating the vertical diffusion depth appears to result in a greater difference in maximum simulated hurricane intensities using the considered approaches.

In addition to hurricane intensity, a consistent trend of hurricane RMW (which represents the hurricane eyewall region), can be seen by altering the eddy diffusivity. As Fig. 9 demonstrates, reducing the vertical diffusion depth (Fig. 9, top right panel) and magnitude (Fig. 9, bottom right panel) leads to a decrease in the simulated hurricane RMW. The largest observed difference is for the YSU runs with $K_m\_lvl_4$ where the $\overline{RMW}_{K_m\_lvl_4\_YSU} = 16\mathrm{km}$ which is half of the unmodified default run's simulated value of $\overline{RMW}_{Default\_YSU} = 32\mathrm{km}$. For the MYJ runs with $K_m\_lvl_4$ modification, the difference in radii of maximum wind speed is $\Delta\overline{RMW}_{K_m\_lvl_4\_MYJ} = 12.8\mathrm{km}$. As for altering the eddy diffusivity magnitude, the results are similar leading to $\Delta\overline{RMW}_{C_k\_0.2\_YSU} = 11.2\mathrm{km}$ and $\Delta\overline{RMW}_{C_k\_0.2\_MYJ} = 14.4\mathrm{km}$ for the YSU and MYJ runs, respectively, when compared to their default unmodified runs. On

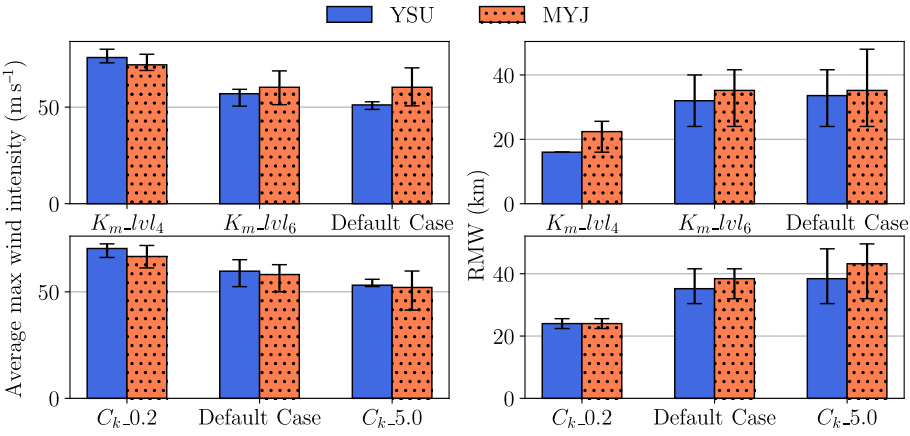

Fig. 9 (Left) The average maximum wind intensity, and (right) the radius of the maximum wind for the YSU (blue) and MYJ (coral) runs with their 20th and 80th percentile error bars. The results are shown as a function of changing the vertical diffusion (top) depth and (bottom) magnitude

the other hand, when increasing the momentum exchange coefficient ($C_k = 5$), the modified simulated hurricanes become weaker ($\Delta\overline{V}_{C_k\_5\_YSU} = -6.5$ m s^{-1}, $\Delta\overline{V}_{C_k\_5\_MYJ} = -6.1$ m s^{-1}), and slightly larger. These trends indicate that altering the vertical diffusion depth and magnitude has a consistent impact on the intensity and size of the considered hurricanes. Moreover, a similar trend was observed when directly modulating the PBL height in the YSU scheme for the simulated hurricanes (see supplementary Fig. S9).

The relationship between the TC intensity and size can be explained using the gradient wind balance. For a given pressure gradient Δp, larger TCs must distribute it over a larger radial distance which leads to a smaller $\partial p \big/ \partial r$. Hence, the pressure gradient from the center to location $r = R$ decreases for larger TCs (smaller $\partial p \big/ \partial r|_{r=R}$), which according to the gradient wind balance, $1/\rho \partial p \big/ \partial r|_{r=R} = f V_g + V_g^2 \big/ R$, implies a smaller gradient wind V_g (Knaff and Zehr 2007). These results are consistent with prior studies that showed smaller vertical diffusion leads to stronger winds, shallower HBL height, and smaller size in simulated TCs (Gopalakrishnan et al. 2013, 2021; Zhang et al. 2015).

3.5 Impacts on Hurricane Intensity, Track, and SLP Forecast Accuracy

In this section, we will characterize the impacts of vertical diffusion modifications on the accuracy of real hurricane forecasts. Our primary focus is on wind intensity improvements; nonetheless, we also provide the performance of the modified runs in terms of track and minimum SLP forecasts. Decreasing the magnitude and depth of the vertical diffusion intensifies the simulated hurricanes. This can be seen in Fig. 10, which depicts the 10 m intensity time series for the considered hurricanes. In the considered cases, decreasing the depth (dashed blue lines in top two rows of Fig. 10) and magnitude (dash-dotted blue lines in bottom two rows of Fig. 10) of K_m as well as the PBL height (dashed turquoise lines in Fig. 10) increased the simulated intensities compared to the default unmodified runs (gray lines). This makes the blue and turquoise lines closer to the black lines which represent the best track NHC data in both considered local and non-local PBL schemes. In all the cases shown, each of the hurricanes undergoes an intensification period, and the magnitude of its 10 m wind intensity increases by at least 17 m s^{-1} in 36 h.

The reduced vertical diffusion cases show a remarkably higher rate of intensification when compared to the unmodified runs. For example, Hurricane Igor ($K_m\_lvl_4\_YSU$, blue line in top right panel of Fig. 10) experiences an increase of $\Delta V_{Igor\_K_m\_lvl_4} \sim 47$ m s^{-1} over a period of 36 h, i.e., an average rate of change of $\Delta V_{Igor\_K_m\_lvl_4}/\Delta t_{simulation} \sim 1.31$ m s^{-1} h^{-1} during the intensification period. When compared to the default run where the average rate of change of intensity is $\Delta V_{Igor\_Default}/\Delta t_{simulation} \sim 0.78$ m s^{-1} h^{-1}, the modified run ($K_m\_lvl_4$, blue line) ends up with a significantly higher 10 m wind intensity of $V_{Igor\_K_m\_lvl_4} = 65$ m s^{-1} in contrast to the $V_{Igor\_Default} = 45.2$ m s^{-1} after a period of 36 h of simulation. Limiting the eddy diffusivity's effective depth to a slightly higher elevation ($K_m\_lvl_6$, green lines in Fig. 10), also improves the intensity forecasts on average albeit less than the $K_m\_lvl_4$ simulations. This is because the average default PBL height in the considered cases is ~ 550 m which is on the same order as in the $K_m\_lvl_6$ cases ~ 536 m and, hence, this change has a smaller impact on simulated TC intensities than $K_m\_lvl_4$.

A similar trend of intensity time series can be seen for modulating the magnitude of the vertical diffusion. Decreasing the vertical turbulent mixing magnitude ($C_k = 0.2$, blue lines in two bottom rows of Fig. 10), produces stronger hurricanes and improves the intensity forecasts compared to the best-observed data and vice versa. For instance, Hurricane Dorian ends up with an increase of $\Delta V_{Dorian\_C_k\_0.2\_YSU} \sim 34.5$ m s^{-1} over a period of 36 h when

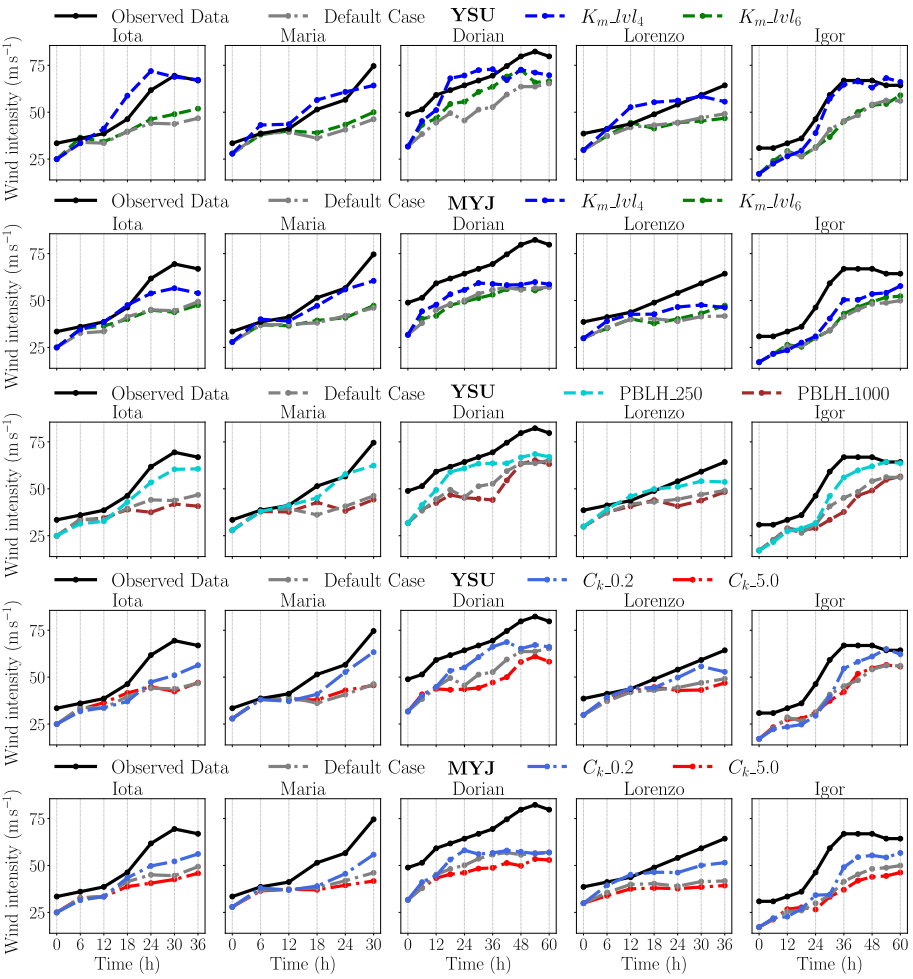

Fig. 10 Time series of the maximum 10 m wind intensities for all hurricane cases with both YSU and MYJ PBL schemes. Black lines represent the best-track observed data, gray lines represent the default simulation runs without modifications. (Top two rows) blue and green dashed lines are simulations with the imposed vertical diffusion depth limiter set at $K_m\_lvl_4$ and $K_m\_lvl_6$. (Middle row) turquoise and brown lines depict the runs with the modified PBL height to $h = 250$ m and $h = 1000$ m, respectively. (Bottom two rows) blue and red dashed-dotted lines represent simulations with modified vertical momentum exchange coefficients C_k_0.2 and C_k_5, respectively

simulated with the YSU PBL scheme and $C_k = 0.2$ (blue line). In terms of the average rate of intensity change, decreasing the magnitude of eddy diffusivity causes ~ 0.96 m s^{-1} h^{-1} which is notably higher than the intensity rate of change for the default (gray line) run ~ 0.58 m s^{-1} h^{-1} and further higher than the one with an increased amount of turbulent mixing (red line) ~ 0.43 m s^{-1} h^{-1}. Therefore, decreasing vertical diffusion magnitude in the considered hurricane simulations improves their intensification period forecasts both for local and non-local PBL schemes.

Unlike hurricane intensity forecasts, predicting track is more challenging since TC tracks are influenced by synoptic and global weather systems and environmental flows that can remarkably modulate them (Roy and Kovordányi 2012; Landsea and Cangialosi 2018; Heming et al. 2019). To examine the impacts of changes in vertical diffusion depth and magnitude on TC track forecasts, we compared them with the best-observed track data provided by NOAA (NOAA-NHC 2021). In general, it is found that the newly implemented vertical diffusion modifications slightly improve track forecasts for considered strong hurricanes. As an example, in Fig. 11 we show a comparison of the forecasted tracks for Hurricanes Dorian and Lorenzo. The upper part of the figure is for the YSU runs with $K_m\_lvl_x$ modifications. Hurricane Dorian's forecasted track improves by $\Delta MAE_{track,Dorian\_YSU} = MAE_{track,Dorian\_Default\_YSU} - MAE_{track,Dorian\_K_m\_lvl_4\_YSU} = 38.2$ km, which yields an improvement of $100\% \times \Delta MAE_{track,Dorian\_YSU}/MAE_{track,Dorian\_Default\_YSU} \sim 58.5\%$ when compared to the default run. Hurricane Lorenzo's forecasted track is enhanced by $\Delta MAE_{track,Lorenzo_YSU} = 15$km which is equivalent to ~ 12.6% improvement. Similar improvements are observed for the MYJ simulation runs as shown in the bottom row of Fig. 11. Furthermore, the traveling velocity of hurricanes is generally increased (e.g., compare blue and gray lines in Fig. 11) and further aligns with the best-observed track. Note that all cases do not have such significant improvements in track forecasts since predicting track is challenging and is affected by many global parameters other than just the vertical turbulent fluxes. The track forecasts of all other considered cases are shown in supplementary material Figs. S12–S14. The average statistical analysis of the track error forecasts for all cases will be shown in Sect. 3.6.

Decreasing the magnitude and depth of the vertical turbulent momentum transport also impacts the minimum SLP of the simulated TCs. Figure 12 shows that generally by decreasing

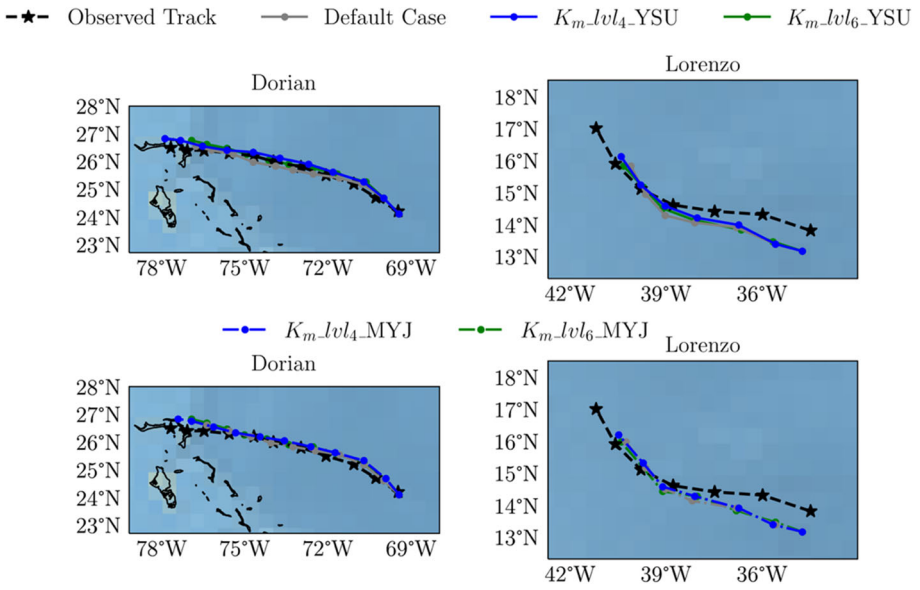

Fig. 11 Simulated and best-observed tracks of Hurricanes Dorian and Lorenzo for (top) the YSU and (bottom) MYJ PBL schemes. The black lines represent the observed track, and the gray lines represent the default simulation runs. Blue and green lines are simulations with vertical diffusion depth limiters set at $K_m\_lvl_4$ and $K_m\_lvl_6$, respectively

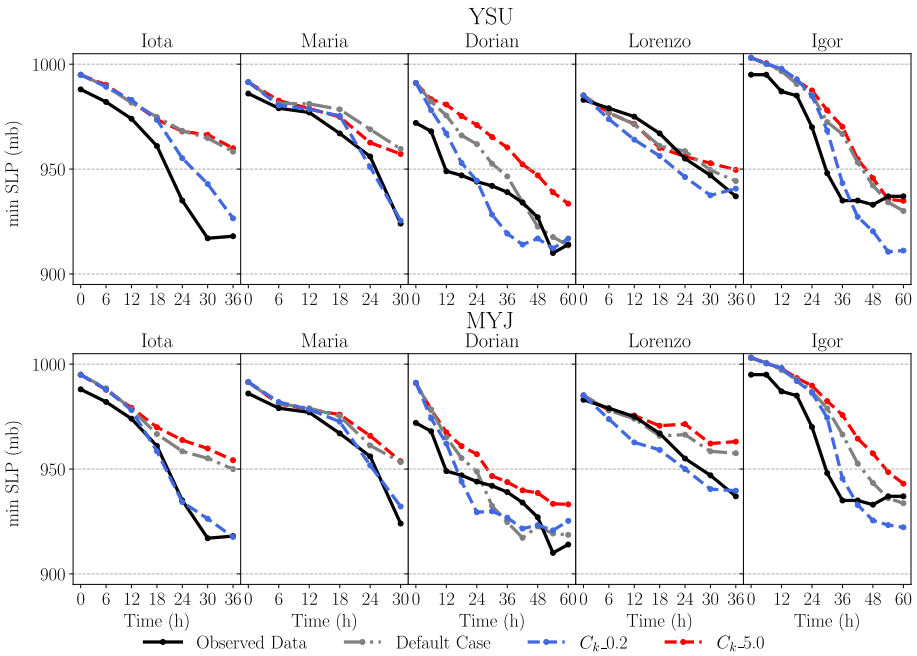

Fig. 12 Time series of the minimum sea-level pressures for five simulated hurricanes using (top) the YSU and (bottom) MYJ PBL schemes. Black lines represent the best observed data and gray lines represent the default simulations. The blue and red lines are runs with modified momentum exchange coefficients C_k_0.2 and C_k_5.0, respectively

the magnitude of the eddy diffusivity (blue lines), the minimum SLP decreases in the considered cases and vice versa. The default simulations overestimate the minimum SLP in some cases (see, e.g., gray lines in Hurricane Iota) compared to the best-observed data (black lines in Fig. 12). On average, the reduced diffusion magnitude cases agree more closely with the best-observed values (see, e.g., blue lines for Hurricanes Iota and Maria runs). Similar trends can be seen when decreasing the depth of the eddy diffusivity in both local and non-local PBL schemes, as well as for reducing the PBL height (please refer to supplementary Figs. S15–S16). On the other hand, when increasing the vertical momentum mixing (red dashed lines in Fig. 12), the storms typically undergo a weaker intensification period, resulting in a lower decrease of minimum SLP (see, e.g., red line in Hurricane Dorian in Fig. 12).

3.6 The Overall Statistics of Improved Hurricane Accuracy of all Considered Cases

To comprehensively assess the impacts of adjusting the vertical diffusion on real hurricane forecasting accuracy, we calculated the intensity, track, and minimum SLP errors of all considered cases. The ensemble average of the forecasting accuracy errors of all vertical diffusion depth modification cases is shown in Fig. 13 for both YSU and MYJ PBL schemes. For the intensity forecasts, on average, a significant improvement of ~ 44.1% is achieved by reducing the vertical diffusion depth in $K_m\_lvl_4\_YSU$ cases (blue bar in Fig. 13a) when compared to the default runs (gray

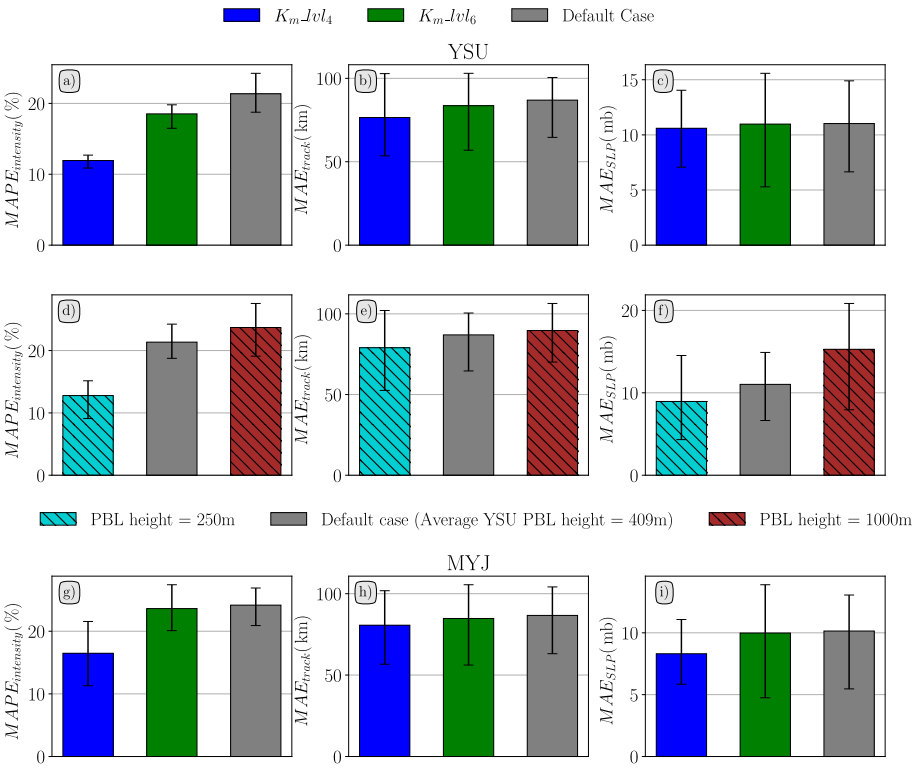

Fig. 13 Ensemble average statistics of reducing the vertical eddy diffusivity depth at two different levels $K_m\_lvl_4$ (blue bars) and $K_m\_lvl_6$ (green bars) for the five considered hurricanes using (a-c) YSU and (g-i) MYJ PBL scheme. (d-f) Another suite of simulations where the PBL height in the YSU scheme is explicitly decreased (turquoise) and increased (brown). From left to right columns represent (a,d,g) normalized wind intensity errors, $MAPE_{intensity}$, (b,e,h) absolute track errors MAE_{track}, and (c,f,i) absolute SLP errors, MAE_{SLP}

bar in Fig. 13a). The improvements are calculated by computing the normalized difference between the modified case performances with the default cases, e.g., as $100\% \times \left[\overline{MAPE_{\text{intensity},Default\_YSU}} - \overline{MAPE_{\text{intensity},K_m\_lvl_4\_YSU}}\right] / \overline{MAPE_{\text{intensity},Default\_YSU}}$. These can also be seen in Table 3, where we summarized the statistics of the forecasted error improvements for intensity and track predictions. For the YSU runs, the highest intensity forecast improvement was observed for Hurricane Dorian with ~ 47.7% improvement, whereas the lowest improvement was observed for Hurricane Lorenzo with ~ 31.4%. As for the MYJ PBL scheme (Fig. 13g), the average $MAPE_{intensity}$ for runs with ($K_m\_lvl_4$) was remarkably improved by ~ 31.8% when compared to the default cases. The highest improvement of ~ 55.3% was noticed for Hurricane Maria, and the lowest improvement of ~ 17.5% was observed for Hurricane Igor.

The primary focus of this paper was on improving the intensity forecasts of strong hurricanes undergoing an intensification period. Nonetheless, by modifying the vertical diffusion depth we also achieved some improvements in track and minimum SLP forecasts albeit the track improvements were small. The middle column of Fig. 13 shows the statistics for MAE_{track}. For the YSU scheme, an average improvement of 12% was achieved for $K_m\_lvl_4$ cases (blue bar in Fig. 13b), when compared to the default simulation runs (gray bar in

Table 3 The summary of the average improvements of $MAPE_{intensity}$ and MAE_{track} of five hurricane cases for three considered PBL modifications

Method	PBL	Average $MAPE_{intensity}$ improvement (%)	Average MAE_{track} improvement (%)
Eddy diffusivity depth, $K_m\_lvl_4$	YSU	44.1	12
	MYJ	31.8	6.9
Eddy diffusivity magnitude, $C_k\_0.2$	YSU	24.9	9
	MYJ	22.2	10.8
$PBL_{height} = 250$ m	YSU	40.1	9.1

Fig. 13b) with the highest improvement for Hurricane Dorian which achieved ~ 58.5% track error reduction. As for the MYJ PBL runs, the average improvement was ~ 6.9% with the highest improvement for Hurricane Dorian of ~ 42.5%. In terms of the minimum SLP forecast improvements, for cases with the YSU PBL scheme (Fig. 13c), on average the improvement was ~ 4% for $K_m\_lvl_4$ cases with the maximum improvement found for Hurricane Iota by ~ 56% when compared to the default runs. For cases with the MYJ PBL scheme (Fig. 13i), on average there was an improvement of ~ 18.1% in minimum SLP forecasts when compared with the default runs.

Modifying the eddy diffusivity effective depth by setting it to zero after a certain height (e.g., $K_m = 0$ after level 4 in $K_m\_lvl_4$ cases) has a similar effect to directly modifying the PBL height. This can be seen from another set of simulations where we explicitly changed the PBL height in the YSU scheme. In this suite of simulations rather than thermodynamically diagnosing the values of h, we set the PBL height to 250 m consistent with previous measurements of HBLs (Zhang et al. 2011b). Note that the average PBL height in the default YSU runs for the five considered hurricanes is ~ 409 m (see supplementary Fig. S17). Thus, setting the PBL height to 250 m reduces the depth of the turbulent boundary layer and eddy diffusivity. Similar results can be seen for the YSU runs when comparing $K_m\_lvl_4$ (blue colors in Fig. 13a–c) with $\text{PBL}_{height} = 250$ m (turquoise colors in Fig. 13d–f) simulations. The vertical profiles of the momentum exchange in Fig. 4 show that in the $K_m\_lvl_4$ cases the effective turbulent boundary layer height is set to vertical level 4, or ≈ 261 m, which is close to $\text{PBL}_{height} = 250$ m cases. Table 3 indicates that the difference in $MAPE_{intensity}$ improvement is only ~ 4% and the difference in MAE_{track} improvement is ~ 2.9% (see also Fig. 13). Therefore, the impacts of modulating the K_m depth and PBL height on TC intensity and track seem to be similar in the considered cases as expected.

We also examined the impacts of increasing the PBL height on hurricane simulations by setting $h = 1000$ m. In Fig. 13(d–f), the brown columns represent the results from runs with $\text{PBL}_{height} = 1000$ m. It can be seen that increasing the default PBL height in the current YSU scheme exacerbates the hurricane forecasts and increases $MAPE_{intensity}$, MAE_{track} and MAE_{SLP} errors. Hence, the results indicate that the current YSU PBL scheme overestimates the vertical diffusion in hurricanes, and reducing it improves hurricane forecasts.

Our last suite of simulations focused on modifying the vertical diffusion magnitude through the control parameter C_k in Eqs. 1–2. Figure 14 shows the overall ensemble average of forecasting accuracy results of adjusting the eddy diffusivity magnitude in five considered hurricanes. When decreasing the magnitude of the vertical diffusion, we observed significant improvements in $MAPE_{intensity}$ for both PBL schemes (blue bars in Fig. 14a,d) compared

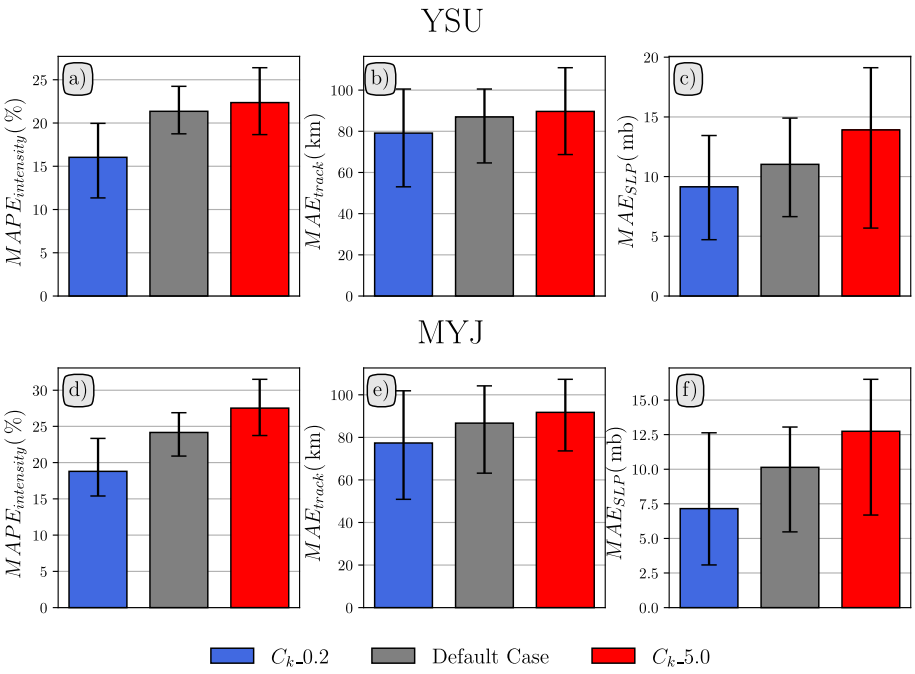

Fig. 14 Ensemble average statistics of varying the momentum exchange coefficient, C_k, for five cases studied in the paper using (top) YSU, and (bottom) MYJ PBL schemes. From left to right columns represent (**a**, **d**) normalized wind intensity error, $MAPE_{intensity}$, (**b**, **e**) absolute track errors, MAE_{track}, and (**c**, **f**) absolute minimum SLP errors, MAE_{SLP}

to the default unmodified runs (gray bars). For the YSU and MYJ PBL schemes, an average improvement of 24.9% (Fig. 14a) and 22.2% (Fig. 14d) with respect to the default runs were achieved, respectively, when decreasing the eddy diffusivity magnitude (C_k_0.2). The summary of error improvement results is also shown in Table 3. The largest improvement for the YSU PBL scheme was for Hurricane Maria with an improved $MAPE_{intensity}$ of ~ 39.1%, and the lowest intensity improvement was for Hurricane Igor with ~ 11.8%. For the MYJ PBL scheme, the reduced diffusion magnitude improved the intensity forecasts of all considered cases between ~ 12–45.5% when compared to their default runs.

The track forecasts were also generally improved by decreasing the default vertical diffusion. As Fig. 14 indicates, on average, decreasing the magnitude of the eddy diffusivity (blue bars in Fig. 14b,e) results in ~ 9% and ~ 10.8% improvements in MAE_{track} compared to the default YSU and MYJ PBL schemes, respectively. The highest track improvements for the modified YSU and MYJ PBL schemes were observed in Hurricane Dorian with ~ 46% and ~ 52.5% enhancements, respectively. Finally, Fig. 14c,f indicates that the minimum SLP forecasts are also considerably improved when decreasing the magnitude of the eddy diffusivity. For the YSU PBL scheme, the MAE_{SLP} was improved by ~ 17.1% on average when compared with the default runs, whereas runs with the modified MYJ PBL scheme led to an even better average improvement of ~ 30%. On the other hand, increasing the magnitude of the default eddy diffusivity (C_k_5.0, red bars in Fig. 14), exacerbated the accuracy of intensity, track, and minimum SLP forecasts on average for the five considered hurricanes.

The results from these simulations demonstrate that the current YSU and MYJ PBL schemes (aka two widely used non-local and local parameterizations in WRF) are overly

diffusive in simulating strong intensifying hurricanes. The reason for this inaccurate PBL parameterization for TCs lies in the fact that the current turbulence closures in WRF do not account for the unique dynamics of hurricane flows. One major overlooked factor in hurricane dynamics is their strong rotation which has a much larger Rossby number ($Ro \gtrsim 1$) compared to regular PBLs ($Ro \sim 0$). Rotation can suppress turbulence production in hurricane flows (Momen et al. 2021; Romdhani et al. 2022) while the effect of strong rotation in TCs has not been considered in current PBL schemes. By adjusting the depth and magnitude of the vertical diffusion, which improved hurricane forecasts, the paper demonstrates this deficiency in current PBL schemes. Our results motivate further studies to comprehensively address this issue in NWPs. One suggested approach is a spatially variable adjustment of eddy diffusivity based on the local angular velocity magnitude following previous engineering applications (Bradshaw 1973; Durbin 2011). This will be done in future work as the main focus of this paper was to extensively establish the existing deficiencies of current PBL schemes in WRF-ARW for forecasting strong hurricanes using systematic suites of simulations and error analysis.

4 Summary

In this study, the impacts of vertical diffusion depth and magnitude on simulated major hurricane dynamics and forecasting accuracy were comprehensively characterized in two widely used local and non-local PBL schemes of the WRF-ARW model. In total, 80 simulations were conducted for five different category 4–5 hurricanes and two different PBL schemes (YSU and MYJ). First, a grid sensitivity analysis was carried out to examine the grid dependence of the default models and to maintain computational efficiency for the next runs. Following the grid dependence test, three different types of analysis were performed by modifying the vertical momentum eddy diffusivity and PBL height. In the first set of simulations (20 runs), the depth of the vertical diffusivity was constrained at a certain vertical level ($K_m\_lvl_4$ and $K_m\_lvl_6$). Another suite of simulations was conducted in which the PBL height was explicitly modified and prescribed in the YSU scheme. In the last batch of runs (20 simulations), the magnitude of the default vertical eddy diffusivity was altered (via $C_k = 0.2$ and $C_k = 5.0$) to determine the impacts of the vertical diffusion strength on hurricane simulations. The key findings of this paper are as follows.

- Decreasing the depth and magnitude of the vertical diffusion in WRF-ARW simulations increases the intensity of the TCs and decreases the size of the vortex. Furthermore, these reductions in the vertical diffusion led to a lower minimum SLP, a shallower but stronger inflow layer, and a smaller radius of maximum wind speed.
- Comparisons with best-observed data indicate that reducing the default depth and magnitude of the eddy diffusivity and PBL height improves the accuracy of strong hurricane forecasts. Decreasing the depth of the eddy diffusivity led to an overall improvement of ~ 44.1% (~ 31.8%) in the forecasted wind intensity and ~ 12% (~ 6.9%) in track forecasts when compared to the default unmodified runs for the YSU (MYJ) PBL scheme. On average, decreasing the PBL height to 250 m (compared to the average ~ 410 m default height in YSU) led to similar results to constraining the vertical eddy diffusivity depth to ~ 260 m.
- Decreasing the magnitude of the default eddy diffusivity ($C_k\_0.2$) also improved the intensity forecasts of the considered hurricanes by ~ 24.9% (~ 22.2%) and their track predictions by ~ 9% (~ 10.8%) when compared to the default YSU (MYJ) PBL cases. Furthermore,

the minimum SLP forecasts enhanced by ~ 17.1% (~ 30.0%) when compared to the default runs in the YSU (MYJ) scheme. An opposite trend was observed when increasing the PBL height and eddy diffusivity magnitude.

- These improvements indicate that both considered local and non-local PBL schemes (YSU and MYJ) in WRF-ARW are overly dissipative for simulating major hurricanes. The reason for this is that strong rotation in hurricanes can suppress turbulence production and lead to lower turbulent stresses and boundary layer heights. However, the impacts of rotation on PBL schemes have not been considered in the current models. Thus, decreasing the default magnitude and depth of the PBL schemes in WRF-ARW substantially improves their forecasting skill for major hurricane flows.

Turbulent mixing in PBLs plays a significant role in determining the dynamics of atmospheric simulations in any NWP model. The current PBL closures in NWPs are typically designed for regular PBLs ($Ro \ll 1$) and do not consider many complexities that exist in real-world PBLs. In this paper, we demonstrated that two frequently used local and non-local PBL schemes in WRF-ARW are overly diffusive for simulating major hurricane flows, and rotational corrections of these schemes need to be considered. These enhancements in PBL parameterizations can lead to improved hurricane intensity and track forecasts in operational NWPs. Such enhanced TC forecasts can reduce some adverse effects of these extreme weather events, e.g., by proper planning and preparation in hurricane-prone regions.

Supplementary Information The online version contains supplementary material available at https://doi.org/10.1007/s10546-023-00818-w.

Author Contributions MM designed research. LM performed research. LM and MM wrote the manuscript text. All authors reviewed the manuscript.

Funding The authors acknowledge support from the Physical and Dynamic Meteorology Program of the National Science Foundation under grant AGS-2228299 as well as the Department of Civil and Environmental Engineering at the University of Houston via startup funds. The simulations were performed on the University of Houston's computing clusters (Carya and Sabine).

Data Availability The data for the observed best tracks and intensity timeseries are already presented in the paper. The data for 8 km resolution simulations of Hurricane Maria can be found in Matak and Momen (2023).

Declarations

Competing interests The authors declare that they have no conflicts of interest.

References

Alimohammadi M, Malakooti H (2018) Sensitivity of simulated cyclone Gonu intensity and track to variety of parameterizations: advanced hurricane WRF model application. J Earth Syst Sci 127:41. https://doi.org/10.1007/s12040-018-0941-4

Arolla SK, Durbin PA (2013) Modeling rotation and curvature effects within scalar eddy viscosity model framework. Int J Heat Fluid Flow 39:78–89. https://doi.org/10.1016/j.ijheatfluidflow.2012.11.006

Beare RJ, Macvean MK, Holtslag AAM et al (2006) An intercomparison of large-eddy simulations of the stable boundary layer. Boundary Layer Meteorol 118:247–272. https://doi.org/10.1007/s10546-004-2820-6

Bhaskar Rao DV, Hari Prasad D, Srinivas D (2009) Impact of horizontal resolution and the advantages of the nested domains approach in the prediction of tropical cyclone intensification and movement. J Geophys Res 114:D11106. https://doi.org/10.1029/2008JD011623

Bhatia KT, Vecchi GA, Knutson TR et al (2019) Recent increases in tropical cyclone intensification rates. Nat Commun 10:635. https://doi.org/10.1038/s41467-019-08471-z

Bradshaw P (1973) Effects Of Streamline Curvature On Turbulent Flow. AGARDograph AG-169
Braun SA, Tao W-K (2000) Sensitivity of high-resolution simulations of hurricane bob (1991) to planetary boundary layer parameterizations. Mon Weather Rev 128:3941–3961. https://doi.org/10.1175/1520-0493(2000)129%3c3941:SOHRSO%3e2.0.CO;2
Bu YP, Fovell RG, Corbosiero KL (2017) The influences of boundary layer mixing and cloud-radiative forcing on tropical cyclone size. J Atmos Sci 74:1273–1292. https://doi.org/10.1175/JAS-D-16-0231.1
Cangialosi JP, Blake E, DeMaria M et al (2020) Recent progress in tropical cyclone intensity forecasting at the national hurricane center. Weather Forecast 35:1913–1922. https://doi.org/10.1175/WAF-D-20-0059.1
Cazalbou J-B, Chassaing P, Dufour G, Carbonneau X (2005) Two-equation modeling of turbulent rotating flows. Phys Fluids 17:055110. https://doi.org/10.1063/1.1920630
Cheikh MI, Momen M (2020) The interacting effects of storm surge intensification and sea-level rise on coastal resiliency: a high-resolution turbulence resolving case study. Environ Res Commun 2:115002. https://doi.org/10.1088/1361-6463/aad7de
Chen X (2022) How do planetary boundary layer schemes perform in hurricane conditions: a comparison with large-eddy simulations. J Adv Model Earth Syst. https://doi.org/10.1029/2022MS003088
Choudhury D, Das S (2017) The sensitivity to the microphysical schemes on the skill of forecasting the track and intensity of tropical cyclones using WRF-ARW model. J Earth Syst Sci 126:57. https://doi.org/10.1007/s12040-017-0830-2
Davis C, Wang W, Dudhia J, Torn R (2010) Does increased horizontal resolution improve hurricane wind forecasts? Weather Forecast 25:1826–1841. https://doi.org/10.1175/2010WAF2222423.1
DeMaria M, Franklin JL, Onderlinde MJ, Kaplan J (2021) Operational forecasting of tropical cyclone rapid intensification at the national hurricane center. Atmosphere 12:683. https://doi.org/10.3390/atmos12060683
Durbin P (2011) Review: adapting scalar turbulence closure models for rotation and curvature. J Fluids Eng. DOI 10(1115/1):4004150
Ek MB, Mitchell KE, Lin Y et al (2003) Implementation of Noah land surface model advances in the national centers for environmental prediction operational mesoscale eta model. J Geophys Res Atmos. https://doi.org/10.1029/2002JD003296
Elsberry RL (2014) Advances in research and forecasting of tropical cyclones from 1963–2013. Asia Pac J Atmos Sci 50:3–16. https://doi.org/10.1007/s13143-014-0001-1
Emanuel KA (1988) The maximum intensity of hurricanes. J Atmos Sci 45:1143–1155
Emanuel K (2005) Increasing destructiveness of tropical cyclones over the past 30 years. Nature 436:686–688. https://doi.org/10.1038/nature03906
Fierro AO, Rogers RF, Marks FD, Nolan DS (2009) The impact of horizontal grid spacing on the microphysical and kinematic structures of strong tropical cyclones simulated with the WRF-ARW model. Mon Weather Rev 137:3717–3743. https://doi.org/10.1175/2009MWR2946.1
Gall R, Franklin J, Marks F et al (2013) The hurricane forecast improvement project. Bull Am Meteorol Soc 94:329–343. https://doi.org/10.1175/BAMS-D-12-00071.1
Gopalakrishnan SG, Goldenberg S, Quirino T et al (2012) Toward improving high-resolution numerical hurricane forecasting: influence of model horizontal grid resolution, initialization, and physics. Weather Forecast 27:647–666. https://doi.org/10.1175/WAF-D-11-00055.1
Gopalakrishnan SG, Marks F, Zhang JA et al (2013) A study of the impacts of vertical diffusion on the structure and intensity of the tropical cyclones using the high-resolution HWRF system. J Atmos Sci 70:524–541. https://doi.org/10.1175/JAS-D-11-0340.1
Gopalakrishnan S, Hazelton A, Zhang JA (2021) Improving hurricane boundary layer parameterization scheme based on observations. Earth Space Sci. https://doi.org/10.1029/2020EA001422
Green BW, Zhang F (2015) Numerical simulations of Hurricane Katrina (2005) in the turbulent gray zone. J Adv Model Earth Syst 7:142–161. https://doi.org/10.1002/2014MS000399
Heming JT, Prates F, Bender MA et al (2019) Review of recent progress in tropical cyclone track forecasting and expression of uncertainties. Trop Cyclone Res Rev 8:181–218. https://doi.org/10.1016/j.tcrr.2020.01.001
Hill KA, Lackmann GM (2009) Analysis of idealized tropical cyclone simulations using the weather research and forecasting model: sensitivity to turbulence parameterization and grid spacing. Mon Weather Rev 137:745–765. https://doi.org/10.1175/2008MWR2220.1
Holtslag AAM, Svensson G, Baas P et al (2013) Stable atmospheric boundary layers and diurnal cycles: challenges for weather and climate models. Bull Am Meteorol Soc 94:1691–1706. https://doi.org/10.1175/BAMS-D-11-00187.1
Hong S-Y (2010) A new stable boundary-layer mixing scheme and its impact on the simulated East Asian summer monsoon. Q J R Meteorol Soc 136:1481–1496. https://doi.org/10.1002/qj.665

Hong S-Y, Lim J-O (2006) The WRF single-monent 6-class microphysics scheme (WSM6). Asia Pac J Atmos Sci 42:129–151
Hong S-Y, Noh Y, Dudhia J (2006) A new vertical diffusion package with an explicit treatment of entrainment processes. Mon Weather Rev 134:2318–2341. https://doi.org/10.1175/MWR3199.1
Huffman GJ, Bolvin DT, Braithwaite D, et al (2015) NASA global precipitation measurement (GPM) integrated multi-satellite retrievals for GPM (IMERG). Algorithm Theoretical Basis Document (ATBD) Version 4:26
Janjić ZI (1994) The step-mountain eta coordinate model: further developments of the convection, viscous sublayer, and turbulence closure schemes. Mon Weather Rev 122:927–945. https://doi.org/10.1175/1520-0493(1994)122%3c0927:TSMECM%3e2.0.CO;2
Janjic Z (2002) Nonsingular Implementation of the Mellor-Yamada Level 2.5 Scheme in the NCEP Meso model. NCEP Office Note 437:
Jin H, Peng MS, Jin Y, Doyle JD (2014) An evaluation of the impact of horizontal resolution on tropical cyclone predictions using COAMPS-TC. Weather Forecast 29:252–270. https://doi.org/10.1175/WAF-D-13-00054.1
Kain JS (2004) The Kain–Fritsch convective parameterization: an update. J Appl Meteorol 43:170–181. https://doi.org/10.1175/1520-0450(2004)043%3c0170:TKCPAU%3e2.0.CO;2
Kanada S, Wada A, Nakano M, Kato T (2012) Effect of planetary boundary layer schemes on the development of intense tropical cyclones using a cloud-resolving model. J Geophys Res Atmos. https://doi.org/10.1029/2011JD016582
Kepert JD (2012) Choosing a boundary layer parameterization for tropical cyclone modeling. Mon Weather Rev 140:1427–1445. https://doi.org/10.1175/MWR-D-11-00217.1
Kidder SQ, Goldberg MD, Zehr RM et al (2000) Satellite Analysis of tropical cyclones using the advanced microwave sounding unit (AMSU). Bull Am Meteorol Soc 81:1241–1259. https://doi.org/10.1175/1520-0477(2000)081%3c1241:SAOTCU%3e2.3.CO;2
Klotz BW, Uhlhorn EW (2014) Improved stepped frequency microwave radiometer tropical cyclone surface winds in heavy precipitation. J Atmos Ocean Technol 31:2392–2408. https://doi.org/10.1175/JTECH-D-14-00028.1
Knaff JA, Zehr RM (2007) Reexamination of tropical cyclone wind-pressure relationships. Weather Forecast 22:71–88. https://doi.org/10.1175/WAF965.1
Kossin JP (2017) Hurricane intensification along United States coast suppressed during active hurricane periods. Nature 541:390–393. https://doi.org/10.1038/nature20783
Krishnamurti TN, Pattnaik S, Stefanova L et al (2005) The hurricane intensity issue. Mon Weather Rev 133:1886–1912. https://doi.org/10.1175/MWR2954.1
Ku J, Kutty G, George B (2020) On the predictability and dynamics of tropical cyclone nargis (2008). J Geophys Res Atmos. https://doi.org/10.1029/2019JD032040
Landsea CW, Cangialosi JP (2018) Have we reached the limits of predictability for tropical cyclone track forecasting? Bull Am Meteorol Soc 99:2237–2243. https://doi.org/10.1175/BAMS-D-17-0136.1
Landsea CW, Franklin JL (2013) Atlantic hurricane database uncertainty and presentation of a new database format. Mon Weather Rev 141:3576–3592. https://doi.org/10.1175/MWR-D-12-00254.1
Li D, Katul GG, Bou-Zeid E (2012) Mean velocity and temperature profiles in a sheared diabatic turbulent boundary layer. Phys Fluid 24:105105. https://doi.org/10.1063/1.4757660
Li S, Chen C, Wu Z et al (2020) Impacts of oceanic mixed layer on hurricanes: a simulation experiment with hurricane sandy. J Geophys Res Oceans. https://doi.org/10.1029/2019JC015851
Li M, Zhang JA, Matak L, Momen M (2023) The impacts of adjusting momentum roughness length on strong and weak hurricanes forecasts: a comprehensive analysis of weather simulations and observations. Mon Weather Rev. https://doi.org/10.1175/MWR-D-22-0191.1
Liu J, Zhang F, Pu Z (2017) Numerical simulation of the rapid intensification of Hurricane Katrina (2005): Sensitivity to boundary layer parameterization schemes. Adv Atmos Sci 34. https://doi.org/10.1007/s00376-016-6209-5
Ma Z, Fei J, Huang X, Cheng X (2018) Sensitivity of the simulated tropical cyclone intensification to the boundary-layer height based on a *k-profile* boundary-layer parameterization scheme. J Adv Model Earth Syst 10:2912–2932. https://doi.org/10.1029/2018MS001459
Matak L, Momen M (2023) The role of vertical diffusion parameterizations in the dynamics and accuracy of simulated intensifying hurricanes. Harvard Dataverse, V1. https://doi.org/10.7910/DVN/NFHOZ8
Mellor GL, Yamada T (1982) Development of a turbulence closure model for geophysical fluid problems. Rev Geophys 20:851. https://doi.org/10.1029/RG020i004p00851
Momen M (2022) Baroclinicity in stable atmospheric boundary layers: characterizing turbulence structures and collapsing wind profiles via reduced models and large-eddy simulations. Q J R Meteorol Soc 148:76–96. https://doi.org/10.1002/qj.4193

Momen M, Bou-Zeid E (2016) Large-eddy simulations and damped-oscillator models of the unsteady ekman boundary layer*. J Atmos Sci 73:25–40. https://doi.org/10.1175/JAS-D-15-0038.1
Momen M, Bou-Zeid E (2017a) Mean and turbulence dynamics in unsteady Ekman boundary layers. J Fluid Mech 816:209–242. https://doi.org/10.1017/jfm.2017.76
Momen M, Bou-Zeid E (2017b) Analytical reduced models for the non-stationary diabatic atmospheric boundary layer. Boundary Layer Meteorol 164:383–399. https://doi.org/10.1007/s10546-017-0247-0
Momen M, Bou-Zeid E, Parlange MB, Giometto M (2018) Modulation of mean wind and turbulence in the atmospheric boundary layer by baroclinicity. J Atmos Sci 75:3797–3821. https://doi.org/10.1175/JAS-D-18-0159.1
Momen M, Parlange MB, Giometto MG (2021) Scrambling and reorientation of classical atmospheric boundary layer turbulence in hurricane winds. Geophys Res Lett. https://doi.org/10.1029/2020GL091695
NOAA-NCEI (2021) NOAA National Centers for Environmental Information (NCEI) U.S. Billion-Dollar Weather and Climate Disasters (2023). https://www.ncei.noaa.gov/access/billions/, DOI: https://doi.org/10.25921/stkw-7w73. Accessed 3 May 2023
NOAA-NHC (2021) Historical Hurricane Tracks. In: National Oceanic and Atmospheric Administration, US Department of Commerce. https://coast.noaa.gov/hurricanes/
Nolan DS, Stern DP, Zhang JA (2009) Evaluation of planetary boundary layer parameterizations in tropical cyclones by comparison of in situ observations and high-resolution simulations of hurricane isabel (2003) Part II Inner-core boundary layer and eyewall structure. Mon Weather Rev. https://doi.org/10.1175/2009MWR2786.1
Nolan DS, Zhang JA, Stern DP (2009b) Evaluation of planetary boundary layer parameterizations in tropical cyclones by comparison of in situ observations and high-resolution simulations of hurricane isabel (2003). part I: initialization, maximum winds, and the outer-core boundary layer. Mon Weather Rev 137:3651–3674. https://doi.org/10.1175/2009MWR2785.1
Pan Y, Follett E, Chamecki M, Nepf H (2014) Strong and weak, unsteady reconfiguration and its impact on turbulence structure within plant canopies. Phys Fluids 26:105102. https://doi.org/10.1063/1.4898395
Pasch RJ, Penny AB, Berg R (2019) National Hurricane Center tropical cyclone report: Hurricane Maria (AL152017). National Hurricane Center
Rajeswari JR, Srinivas CV, Mohan PR, Venkatraman B (2020) Impact of boundary layer physics on tropical cyclone simulations in the bay of bengal using the WRF model. Pure Appl Geophys 177:5523–5550. https://doi.org/10.1007/s00024-020-02572-3
Ramamurthy P, Pardyjak ER, Klewicki JC (2007) Observations of the effects of atmospheric stability on turbulence statistics deep within an urban street canyon. J Appl Meteorol Climatol 46:2074–2085. https://doi.org/10.1175/2007JAMC1296.1
Rios-Berrios R, Torn RD (2017) Climatological analysis of tropical cyclone intensity changes under moderate vertical wind shear. Mon Weather Rev 145:1717–1738. https://doi.org/10.1175/MWR-D-16-0350.1
Romdhani O, Zhang JA, Momen M (2022) Characterizing the impacts of turbulence closures on real hurricane forecasts: a comprehensive joint assessment of grid resolution, horizontal turbulence models, and horizontal mixing length. J Adv Model Earth Syst. https://doi.org/10.1029/2021MS002796
Roy C, Kovordányi R (2012) Tropical cyclone track forecasting techniques—a review. Atmos Res 104–105:40–69. https://doi.org/10.1016/j.atmosres.2011.09.012
Sabet F, Yi YR, Thomas L, Momen M (2022) Characterizing mean and turbulent structures of hurricane winds via large-eddy simulations. Center Turbul Res Proc Summer Progr 2022:311–321
Salesky ST, Anderson W (2018) Buoyancy effects on large-scale motions in convective atmospheric boundary layers: implications for modulation of near-wall processes. J Fluid Mech 856:135–168. https://doi.org/10.1017/jfm.2018.711
Salesky ST, Chamecki M, Bou-Zeid E (2017) On the nature of the transition between roll and cellular organization in the convective boundary layer. Boundary Layer Meteorol 163:41–68. https://doi.org/10.1007/s10546-016-0220-3
Shen F, Min J, Xu D (2016) Assimilation of radar radial velocity data with the WRF Hybrid ETKF-3DVAR system for the prediction of Hurricane Ike (2008). Atmos Res 169
Shen F, Xu D, Min J et al (2020) Assimilation of radar radial velocity data with the WRF hybrid 4DEnVar system for the prediction of hurricane Ike (2008). Atmos Res 234. https://doi.org/10.1016/j.atmosres.2019.104771
Shin HH, Dudhia J (2016) Evaluation of PBL parameterizations in WRF at subkilometer grid spacings: turbulence statistics in the dry convective boundary layer. Mon Weather Rev 144:1161–1177. https://doi.org/10.1175/MWR-D-15-0208.1
Simpson H, Saffir H (1974) The hurricane disaster—potential scale. Weatherwise 27:169–186. https://doi.org/10.1080/00431672.1974.9931702

Skamarock WC, Klemp JB, Dudhia JB et al (2021) A Description of the Advanced Research WRF Model Version 4.3. NCAR Tech Note. https://doi.org/10.5065/1dfh-6p97
Skamarock WC et al. (2008) A description of the advanced research WRF version 3, NCAR Tech. Note, NCAR/TN-468+STR. Natl Cent for Atmos Res Boulder, Colorado
Smith RK, Montgomery MT (2010) Hurricane boundary-layer theory. Q J R Meteorol Soc 136:1665–1670. https://doi.org/10.1002/qj.679
Srinivas CV, Bhaskar Rao DV, Yesubabu V et al (2013) Tropical cyclone predictions over the bay of bengal using the high-resolution advanced research weather research and forecasting (ARW) model. Q J R Meteorol Soc. https://doi.org/10.1002/qj.2064
Stoll R, Gibbs JA, Salesky ST et al (2020) Large-eddy simulation of the atmospheric boundary layer. Boundary Layer Meteorol 177:541–581. https://doi.org/10.1007/s10546-020-00556-3
Stull R (1988) An Introduction to Boundary Layer Meteorology, 1st edn. Kluwer Academic Publishers, Dordrecht
Tritton DJ (1992) Stabilization and destabilization of turbulent shear flow in a rotating fluid. J Fluid Mech 241:503–523. https://doi.org/10.1017/S0022112092002131
U.S. Global Change Research Program (2017) Climate Science Special Report: Fourth National Climate Assessment, Volume I. Washington, DC
van de Wiel BJH, Moene AF, Steeneveld GJ et al (2010) A conceptual view on inertial oscillations and nocturnal low-level jets. J Atmos Sci 67:2679–2689. https://doi.org/10.1175/2010JAS3289.1
van de Wiel BJH, Moene AF, Jonker HJJ (2012) The cessation of continuous turbulence as precursor of the very stable nocturnal boundary layer. J Atmos Sci 69:3097–3115. https://doi.org/10.1175/JAS-D-12-064.1
Wei W, Bruyère C, Duda M, et al (2019) WRF ARW version 4 modeling system user's guide
Worsnop RP, Bryan GH, Lundquist JK, Zhang JA (2017) Using large-eddy simulations to define spectral and coherence characteristics of the hurricane boundary layer for wind-energy applications. Boundary Layer Meteorol 165:55–86. https://doi.org/10.1007/s10546-017-0266-x
Zhang JA (2010) Spectral characteristics of turbulence in the hurricane boundary layer over the ocean between the outer rain bands. Q J R Meteorol Soc 136:918–926. https://doi.org/10.1002/qj.610
Zhang JA, Drennan WM (2012) An observational study of vertical eddy diffusivity in the hurricane boundary layer. J Atmos Sci. https://doi.org/10.1175/JAS-D-11-0348.1
Zhang JA, Rogers RF (2019) Effects of parameterized boundary layer structure on hurricane rapid intensification in shear. Mon Weather Rev 147:853–871. https://doi.org/10.1175/MWR-D-18-0010.1
Zhang JA, Drennan WM, Black PG, French JR (2009) Turbulence structure of the hurricane boundary layer between the outer rainbands. J Atmos Sci 66:2455–2467. https://doi.org/10.1175/2009JAS2954.1
Zhang JA, Marks FD, Montgomery MT, Lorsolo S (2011a) An estimation of turbulent characteristics in the low-level region of intense hurricanes Allen (1980) and Hugo (1989). Mon Weather Rev 139:1447–1462. https://doi.org/10.1175/2010MWR3435.1
Zhang JA, Rogers RF, Nolan DS, Marks FD (2011b) On the characteristic height scales of the hurricane boundary layer. Mon Weather Rev 139:2523–2535. https://doi.org/10.1175/MWR-D-10-05017.1
Zhang JA, Nolan DS, Rogers RF, Tallapragada V (2015) Evaluating the Impact of Improvements in the boundary layer parameterization on hurricane intensity and structure forecasts in HWRF. Mon Weather Rev 143:3136–3155. https://doi.org/10.1175/MWR-D-14-00339.1
Zhang JA, Rogers RF, Tallapragada V (2017) Impact of parameterized boundary layer structure on tropical cyclone rapid intensification forecasts in HWRF. Mon Weather Rev 145:1413–1426. https://doi.org/10.1175/MWR-D-16-0129.1
Zhang JA, Kalina EA, Biswas MK et al (2020) A review and evaluation of planetary boundary layer parameterizations in hurricane weather research and forecasting model using idealized simulations and observations. Atmosphere 11:1091. https://doi.org/10.3390/atmos11101091